Behavioral/Cognitive

Tonic Inhibition of Accumbal Spiny Neurons by Extrasynaptic $\alpha 4\beta\delta$ GABA$_A$ Receptors Modulates the Actions of Psychostimulants

Edward P. Maguire,[1]* Tom Macpherson,[2]* Jerome D. Swinny,[3]* Claire I. Dixon,[2] Murray B. Herd,[1] Delia Belelli,[1] David N. Stephens,[2] Sarah L. King,[2]† and Jeremy J. Lambert[2]†

[1]Division of Neuroscience, Medical Research Institute, Ninewells Hospital and Medical School, Ninewells Hospital, Dundee University, Dundee, DD19SY, United Kingdom, [2]School of Psychology, University of Sussex, Falmer, Brighton, BN1 9QG, United Kingdom, and [3]Institute for Biomedical and Biomolecular Sciences, School of Pharmacy and Biomedical Sciences, University of Portsmouth, Portsmouth PO1 2DT, United Kingdom

Within the nucleus accumbens (NAc), synaptic GABA$_A$ receptors (GABA$_A$Rs) mediate phasic inhibition of medium spiny neurons (MSNs) and influence behavioral responses to cocaine. We demonstrate that both dopamine D1- and D2-receptor-expressing MSNs (D-MSNs) additionally harbor extrasynaptic GABA$_A$Rs incorporating $\alpha 4$, β, and δ subunits that mediate tonic inhibition, thereby influencing neuronal excitability. Both the selective δ-GABA$_A$R agonist THIP and DS2, a selective positive allosteric modulator, greatly increased the tonic current of all MSNs from wild-type (WT), but not from $\delta^{-/-}$ or $\alpha 4^{-/-}$ mice. Coupling dopamine and tonic inhibition, the acute activation of D1 receptors (by a selective agonist or indirectly by amphetamine) greatly enhanced tonic inhibition in D1-MSNs but not D2-MSNs. In contrast, prolonged D2 receptor activation modestly reduced the tonic conductance of D2-MSNs. Behaviorally, WT and constitutive $\alpha 4^{-/-}$ mice did not differ in their expression of cocaine-conditioned place preference (CPP). Importantly, however, mice with the $\alpha 4$ deletion specific to D1-expressing neurons ($\alpha 4^{D1-/-}$) showed increased CPP. Furthermore, THIP administered systemically or directly into the NAc of WT, but not $\alpha 4^{-/-}$ or $\alpha 4^{D1-/-}$ mice, blocked cocaine enhancement of CPP. In comparison, $\alpha 4^{D2-/-}$ mice exhibited normal CPP, but no cocaine enhancement. In conclusion, dopamine modulation of GABAergic tonic inhibition of D1- and D2-MSNs provides an intrinsic mechanism to differentially affect their excitability in response to psychostimulants and thereby influence their ability to potentiate conditioned reward. Therefore, $\alpha 4\beta\delta$ GABA$_A$Rs may represent a viable target for the development of novel therapeutics to better understand and influence addictive behaviors.

Key words: addiction; GABA$_A$ receptors; gaboxadol; nucleus accumbens; THIP

Introduction

The nucleus accumbens (NAc) is an important brain region for understanding addictions. Dopaminergic innervation of NAc encouraged dopamine-centered theories of reward and motivation

(Robinson and Berridge, 1993; Everitt et al., 2001; Wise, 2004). However, the NAc consists primarily of GABAergic neurons, so elucidating the role of GABA is essential to better comprehend the neurobiology of reward and addiction.

Many of GABA's effects are mediated by GABA$_A$ receptors (GABA$_A$Rs), which are composed of five subunits drawn from a repertoire of 19 proteins underpinning the expression of multiple receptor isoforms. Subunit composition influences receptor location, pharmacology, and function (Sieghart, 2006; Olsen and Sieghart, 2008; Rudolph and Knoflach, 2011). Determining which GABA$_A$Rs are expressed in the NAc and their role in behavior and addiction is warranted. Medium spiny neurons (MSNs) comprise ~95% of NAc neurons. We demonstrated that NAc core MSNs express synaptic GABA$_A$Rs composed of $\alpha 2$, β, and $\gamma 2$ subunits, which mediate phasic inhibition and are necessary and sufficient for behavioral sensitization to cocaine (Morris et al., 2008; Dixon et al., 2010). In addition, an involvement of NAc GABA$_A$Rs containing $\alpha 4$ and δ subunits in addictive processes is suggested because suppressing their expression reduced ethanol consumption and preference in rats (Nie et al., 2011; Rewal et al., 2012). Furthermore, chronic cocaine robustly increases $\alpha 4$-subunit gene expression selectively in D1-MSNs (Heiman et al., 2008). In thalamus and hippocampus, $\alpha 4\beta\delta$ re-

ceptors are located extra- or perisynaptically and are activated by ambient, or "spillover," GABA to mediate a tonic conductance, which influences excitability (Belelli et al., 2005; Farrant and Nusser, 2005; Brickley and Mody, 2012; Herd et al., 2013; Wlodarczyk et al., 2013). However, in the NAc, their location, function, and how they influence addictive behaviors is not known.

MSNs comprise two broad classes expressing dopamine receptor 1 (D1) or 2 (D2), corresponding primarily to the direct and indirect output pathway neurons, respectively (Gerfen et al., 1990; Smith et al., 2013). We reveal that, in mouse NAc, both D1- and D2-MSNs express $\alpha4\beta\delta$ GABA$_A$Rs that mediate a tonic current, limiting MSN excitability. Acute or prolonged D1-receptor activation by a selective agonist or indirectly by amphetamine greatly increased the tonic conductance of D1-MSNs. In contrast, prolonged D2-receptor activation modestly decreased the corresponding conductance of D2-MSNs. Therefore, $\alpha4\beta\delta$ GABA$_A$Rs may dynamically contribute to the effects of dopamine and consequently certain drugs of abuse. Mice with a specific deletion of the $\alpha4$ subunit from D1-expressing neurons showed greater cocaine-induced conditioned place preference (CPP), whereas activation of these receptors by THIP (4,5,6,7-tetrahydroisoxazolo[4,5-c]pyridine-3-ol/gaboxadol) selectively in the NAc blocked cocaine enhancement of CPP. Mice with a specific deletion of the $\alpha4$ subunit from D2-expressing neurons exhibited normal CPP, but no cocaine enhancement of performance.

In summary, dopamine differentially regulates the activity of $\alpha4\beta\delta$ GABA$_A$Rs on D1- and D2-MSNs and these receptors mediate dissociable pathway-specific influences on cocaine-facilitation of conditioned behaviors. Selective positive allosteric modulators (PAMs) of δ-GABA$_A$Rs (Wafford et al., 2009; Jensen et al., 2013), coupled with genetic manipulation, offer new approaches to explore the role of extrasynaptic GABA$_A$Rs in reward circuitry.

Materials and Methods

Animals
Colonies of mice were maintained at the University of Dundee and the University of Sussex. In both locations, a 12 h light/dark cycle was used, with lights on at 7:00 A.M. and the temperature controlled at 21 ± 2°C and humidity at 50 ± 5%. All procedures were conducted in accordance with the Animals (Scientific Procedures) Act of 1986 after ethical review by the University of Sussex or the University of Dundee Ethical Review Committee. Constitutive $\alpha4$ knock-out ($\alpha4^{-/-}$) mice were produced at the University of Sussex by crossing "floxed $\alpha4$" mice (strain name; B6.129-Gabra4$^{tm1.2Geh}$/J; Jackson Laboratory; Chandra et al., 2006) with Cre-recombinase expressing transgenic mice (strain name; B6.FVB-Tg(Ella-cre)C5379Lmgd/J; Jackson Laboratory). Heterozygous mice were bred to generate $\alpha4^{-/-}$ and wild-type (WT) littermate controls for behavioral experiments. To produce cell-specific knock-out mice, BAC D1- and D2-CRE mice [MMRRC strains B6.FVB(Cg)-Tg(Drd1a-cre)EY266Gsat/Mmucd and B6.FVB(Cg)-Tg(Drd2-cre)ER44Gsat/Mmucd, respectively; Gong et al., 2007], were independently bred into homozygous "floxed" $\alpha4$ mice. Pairs of these homozygous "floxed $\alpha4$" mice, one hemizygous for the BAC transgene and one not, were bred to generate offspring for behavioral experiments (WT: "floxed $\alpha4$" mice and knock-outs $\alpha4^{D1-/-}$ or $\alpha4^{D2-/-}$: "floxed $\alpha4$" mice carrying the BAC D1- or D2-CRE transgenes, respectively). For electrophysiological and immunohistochemical studies, the $\alpha4^{-/-}$, $\delta^{-/-}$, and WT mice were originally generated on a C57BL/6 background at the University of Pittsburgh as described previously (Mihalek et al., 1999; Chandra et al., 2006). Experiments were conducted on the first two generations of WT, $\alpha4^{-/-}$, and $\delta^{-/-}$ breeding pairs derived from the corresponding heterozygous mice bred at the University of Dundee. BAC D1- and BAC D2-EGFP mice (obtained from E. Schmidt, Rockefeller University, New York, NY; Gong et al., 2003) were crossed with C57BL/6J mice. Hemizygous mice

were paired with their WT counterparts to produce offspring. At weaning, all mice were genotyped using PCR.

Immunohistochemistry
Immunohistochemical data were derived from 4 adult (6–8 weeks of age) C57BL/6 male mice, 2 GABA$_A$R $\delta^{-/-}$, 2 GABA$_A$R $\alpha4^{-/-}$, and 2 hemizygous D1-EGFP or D2-EGFP BAC transgenic mice. The immunohistochemical protocols were as described previously (Corteen et al., 2011). Briefly, anesthetized animals were first transcardially perfused with an 0.9% saline solution for 3 minutes, followed by a 12 minute fixation with a fixative consisting of 1% paraformaldehyde and 15% v/v saturated picric acid in 0.1 M phosphate buffer (PB), pH 7.4. The brains were kept in the same fixative solution overnight at 4°C, after which 50-μm-thick coronal sections of the striatum were prepared on a Vibratome.

For antigen retrieval, tissue sections were incubated at 37°C for 10 minutes in 0.1 M PB, followed by 15 minutes in 0.2 M HCl containing 1 mg/ml pepsin (Sigma), and then washed thoroughly in Tris-buffered saline containing 0.3% Triton X-100 (TBS-Tx) for 30 min (Watanabe et al., 1998). The nonspecific binding of secondary antibodies was blocked by incubating sections with 20% normal horse serum for 2 hours at room temperature. The tissue sections were incubated with mixtures of primary antibodies (Table 1), diluted in TBS-Tx, for 24 hours at 4°C. After washing with TBS-Tx, sections were incubated in a mixture of appropriate secondary antibodies conjugated with Alexa Fluor 488 (Invitrogen), indocarbocyanine (Cy3; Jackson ImmunoResearch), or indodicarbocyanine (Cy5; Jackson ImmunoResearch) for 2 hours at room temperature. Sections were washed in TBS-Tx and mounted in Vectashield (Vector Laboratories). The specificity of the antisera against the GABA$_A$R subunits used in this study was confirmed in tissue from GABA$_A$R $\delta^{-/-}$ or $\alpha4^{-/-}$ mice to confirm the authenticity of the signal under our reaction conditions. Method specificity was also tested by omitting the primary antibodies in the incubation sequence. To confirm the absence of cross reactivity between IgGs in double- and triple-immunolabeling experiments, some sections were processed through the same immunocytochemical sequence except that only an individual primary antibody was applied with the full complement of secondary antibodies.

Image acquisition
Sections were examined with a confocal laser-scanning microscope (LSM710; Zeiss) using either a Plan Apochromatic 63× differential interference contrast (DIC) oil objective (numerical aperture [NA] 1.4) or a Plan Apochromatic 100× DIC oil objective (NA1.46). Z-stacks were used for routine evaluation of the labeling. All images presented represent a single optical section. These images were acquired using sequential acquisition of the different channels to avoid cross talk between fluorophores, with the pinholes adjusted to one airy unit. Images were processed with the software Zen 2009 Light Edition (Zeiss) and exported into Adobe Photoshop. Only brightness and contrast were adjusted for the whole frame and no part of a frame was enhanced or modified in any way.

Brain slice preparation, electrophysiology, and analysis
Coronal slices (300 μm) incorporating the NAc (Dixon et al., 2010) were prepared from adult male (2–6 months) $\alpha4^{-/-}$, $\delta^{-/-}$, and hemizygous BAC D1- and BAC D2-EGFP mice and their corresponding WT littermates. The tissue was maintained briefly in oxygenated ice-cold solution containing the following (in mM): 140 K gluconate, 15 Na gluconate, 4 NaCl, 10 HEPES, and 0.2 EGTA, pH 7.2, 310–320 mOsm, during the slice preparation (Dugué et al., 2005) and then stored for ≥1 h (20–23°C) in oxygenated, extracellular solution (ECS) containing the following (in mM): 126 NaCl, 2.95 KCl, 26 NaHCO$_3$, 1.25 NaH$_2$PO$_4$, 2 CaCl$_2$, 10 D-glucose and 2 MgCl$_2$, pH 7.4, 300–310 mOsm. MSNs were identified with an Olympus BX51 microscope equipped with DIC/infrared optics. For experiments using the BAC D1- or the BAC D2-EGFP mice (Gong et al., 2003), a CoolLED system was used to excite—and fluorescent filters optimized to detect—EGFP fluorescence. When BAC D1- or BAC D2-EGFP mice were used for electrophysiology, MSNs were defined as D1 or D2 positive, respectively, based on their expression of

Table 1. Antibodies used in the study

	Species (raised in)	Source/code	Dilution	Specificity reference
Primary antibodies				
Calretinin	Mouse	Swant #6B3	1: 2000	Zimmermann and Schwaller (2002)
DARPP-32	Goat	Santa Cruz Biotechnology #8483	1:250	Labeling pattern as published with other antibodies
Choline acetyl transferase	Goat	Millipore #144P	1: 2000	Labeling pattern as published with other antibodies
		Werner Sieghart antigen sequence, α_{4N} amino acids 1–9		
GABA$_A$ α4 subunit	Rabbit	Rabbit #21/7, bleed #04/10/1999	1:1000	Knock-out mouse, this study
		Werner Sieghart		
		Antigen sequence δ_N amino acids 1–11		
		Rabbit #14/15		
GABA$_A$ δ subunit	Rabbit	Bleed #17/04/1997	1:500	Knock-out mouse, this study
Kv2.1	Mouse	Neuromab #73–014	1:1000	Knock-out mouse, supplier
MAP-2	Mouse	Aves Labs #MAP	1:500	Labeling pattern as published with other antibodies
Neuroligin 2	Rabbit	Synaptic Systems #129 203	1:1000	Labeling pattern as published with other antibodies
Neuroligin 2	Guinea pig	Frontiers Science #Nlgn2-GP-Af760	1:250	Labeling pattern as published with other antibodies
NPY	Mouse	Sigma #WH0004852M1	1:1000	Labeling pattern as published with other antibodies
Parvalbumin	Mouse	Swant #235	1:5000	Knock-out mouse, supplier
Somatostatin	Mouse	GeneTex #GTX71935	1: 500	Labeling pattern as published with other antibodies
Secondary antibodies				
Species		Fluorophore	Dilution	Source code
Donkey anti-rabbit		Alexa Fluor 488 carboxylic acid	1:1000	Life Technologies #A-21206
Donkey anti-goat		Cy3 bis-NHS ester	1:1000	Jackson ImmunoResearch #705-165-147
Donkey anti-mouse		Cy3 bis-NHS ester	1:1000	Jackson ImmunoResearch #715-165-151
Donkey anti-guinea pig		Alexa Fluor 647 carboxylic acid	1:500	Jackson ImmunoResearch #706-605-148
Donkey anti-goat		DyLight 649-TFP ester	1:500	Jackson ImmunoResearch #705-495-147
Donkey anti-mouse		DyLight 649-TFP ester	1:500	Jackson ImmunoResearch #715-495-151

EGFP. Alternatively, the majority of experiments used D1-EGFP mice and recordings from EGFP-negative cells were presumed to represent D2-expressing MSNs (Ade et al., 2008). In some experiments with non-reporter mice, the identity of MSNs was confirmed by their characteristic firing pattern (delayed, repetitive, nonadapting) in response to current injection in current-clamp experiments (Ade et al., 2008; Santhakumar et al., 2010).

Whole-cell voltage-clamp recordings from MSNs were made at 35°C (−60 mV) using ECS supplemented with strychnine (1 μM), kynurenic acid (2 mM), and tetrodotoxin (TTX; 0.5 μM) to inhibit ionotropic glycine, glutamate receptors, and voltage-gated sodium channels, respectively. In some experiments to study spontaneous IPSCs (sIPSCs), TTX was omitted. Recording electrodes (3–4 MΩ) were filled with the following (in mM): 135 CsCl, 10 HEPES, 10 EGTA, 1 CaCl$_2$, 2 MgCl$_2$, 2 Mg-ATP, and 5 QX-314, pH 7.2–7.3 with CsOH, 300–308 mOsm.

Recordings were made from MSNs located within the core region of the NAc and were discarded if the series resistance changed >20%. Currents were filtered at 2 kHz (8-pole, low-pass Bessel filter) and recorded directly to a computer (Dell) using an A/D converter (NIDAQmx; National Instruments) at a 10 kHz sampling rate before analysis (WinEDR/WinWCP; J. Dempster, University of Strathclyde, Glasgow, Scotland). The mIPSCs and, in some experiments sIPSCs, were threshold detected (−4 pA, duration 3 ms) and visually inspected. For mIPSCs, a minimum of 40 events per MSN were used for analysis, including peak amplitude, rise time (10–90%, ≤1 ms), and decay time. The decay phase of averaged mIPSCs was best fit (98–5% of the peak amplitude) with a biexponential $[y(t) = A_{fast} \cdot e^{(-t/\tau fast)} + A_{slow} \cdot e^{(-t/\tau slow)}]$ function, where t is time, A is the amplitude, and τ is the decay time constant. A weighted decay time constant (τ_w) was calculated from: $\tau_w = \tau_1 P_1 + \tau_2 P_2$, where τ_1 and τ_2 are decay time constants and P_1 and P_2 are the relative proportions of the decay described by each component. The mIPSC and sIPSC frequency was determined in 20 s bins for 2 min, with events being detected by the rate of their rise (30–50 pA ms^{-1}).

To investigate the tonic current, the mean current and the associated root mean square were calculated over 102.4 ms epochs for 1 min using a 10 kHz sampling rate (Belelli et al., 2005). Epochs containing mIPSCs or unstable baselines were excluded. To ensure that changes in the holding current reflected a drug effect, 2 control, 1-minute holding-current periods (C1 and C2) were sampled, followed by a 1-minute section after

drug equilibration (D). The mean holding current for C1 and C2 were pooled and the SD calculated. The drug effect was accepted if the absolute change in the holding current (D − C2) was greater than twice the SD of the controls (C1, C2).

To determine the resting membrane potential (RMP) and the GABA$_A$R-mediated Cl$^-$ reversal potential (E_{GABA}) of MSNs, perforated patch recordings were performed at 30°C. Patch electrodes were prepared as for voltage-clamp experiments and had open tip resistances of 4–5 MΩ when filled with a solution containing the following (in mM): 145 KCl, 1 MgCl$_2$, 0.1 CaCl$_2$, 1 EGTA, and 10 HEPES, pH 7.2–7.3 with KOH, 290 mOsm. The gramicidin-based perforated patch configuration (Kyrozis and Reichling, 1995) that maintains the physiological transmembrane Cl$^-$ gradient was achieved by supplementing the prefiltered pipette solution with 12.5–25 μg/ml gramicidin (Sigma-RBI) diluted from a fresh 25 mg/ml stock solution in DMSO. The gramicidin-containing pipette solution was sonicated for 2 minutes before experimentation and further vortexed between each recording attempt. Electrode tips were filled with gramicidin-free solution and subsequently back filled with the antibiotic-containing solution. Perforation was monitored in voltage-clamp mode (holding potential −60 mV) by observing the slow development of capacitive transients in response to −5 mV hyperpolarizing current steps. Full perforation (series resistance <60 MΩ) was generally achieved within 30 minutes The estimated liquid junction potential of 3.4 mV (calculated using pClamp version 8.2) was left uncorrected. To measure E_{GABA}, GABA-evoked responses were recorded under voltage-clamp conditions at holding potentials ranging from −100 to −50 mV (10 mV increments). GABA (1 mM) was focally applied to MSNs from a locally positioned (30–40 μm from the cell soma) pipette coupled to a "Picospritzer II" system, allowing pressure ejection of the agonist (10 ms duration, 7–10 psi; General Valve). Pressure ejection of GABA-free extracellular solution confirmed the lack of any stimulus artifact when using these parameters. The RMP of MSNs was subsequently determined in current-clamp conditions and GABA-evoked responses were also acquired, to confirm the E_{GABA} values determined in voltage-clamp conditions.

Whole-cell current-clamp recordings were made at 30°C in ECS containing no drugs. Patch electrodes were filled with a potassium methane sulfonate-based ICS composed of the following (in mM): 135 KMeSO$_4$, 10 HEPES, 5 KCl, 5 phosphocreatine, 2 MgCl$_2$, 2 Mg-ATP, 0.5 Na-GTP,

and 0.4 EGTA, pH 7.2 with KOH. Employing this intracellular solution and the ECS described above gives a calculated reversal potential for GABA (E_{GABA}) of -71 mV, similar to that obtained in the perforated patch experiments (see Results, Effect THIP and DS2 on MSNs). The liquid junction potential was -11 mV (calculated from pClamp version 10). To estimate the impact of THIP and genotype upon the excitability of NAc MSNs, input-output curves determining the number of action potentials fired in response to current injection were constructed. In current-clamp mode, a stimulus protocol was run to inject current pulses that increased sequentially from $+20$ pA to $+200$ pA in 20 pA steps of 400 ms duration. The membrane potential was adjusted to -87 mV (accounting for the junction potential), a value similar to that determined from the perforated patch experiments.

Behavioral studies
Stereotaxic surgery. Male mice weighing between 20 and 30 g were housed in groups of 2–3 with food and water available *ad libitum*. They were anesthetized with isoflurane and implanted stereotaxically with guide cannulae (26 gauge, 10 mm) directed to NAc (coordinates AP1.34; L+/− 1.00; DV −3.20; (Paxinos and Franklin, 2001). After surgery, mice were singly housed and underwent a 1 week recovery/habituation period. A steel infuser (33 gauge, 11 mm) connected via polyvinyl tubing to a (5 μl) Hamilton Gastight syringe was used to infuse 0.5 μl of either saline or THIP (3 mM) bilaterally for 90 seconds and left to settle for 90 seconds before the infusers were removed. The location of cannulae was confirmed histologically.

Conditioned place preference. CPP was conducted using three-chamber place-conditioning apparatus (outer two conditioning chambers measured 200 × 200 × 200 mm and separated by a central chamber measuring 200 × 50 × 200 mm; Mead et al., 1999). One conditioning chamber was white with meshed metal flooring. The other chamber was black and white (each wall was split along the diagonal, with the top and bottom halves colored black and white, respectively) with a smooth, clear Perspex floor. During the conditioning phase, clear doors were inserted into the outer chambers to restrict movement between chambers via the central chamber. The movement and location of animals was recorded using infrared beam breaks (Mead et al., 1999). Animals received saline injections in their home cages the day before the first experimental session, after which the experiment was divided into three phases. For the pre-conditioning phase (day 1), mice were allowed free access to the apparatus for 20 minutes, during which the time in each chamber was measured to exclude the possibility of a chamber bias. Preconditioning tests of CPP found no bias in preference for the two outer chambers for any genotype in any experiment. For the conditioning phase (days 2–11), mice were administered cocaine (10 mg/kg, i.p.) and confined to one of the outer chambers for 40 minutes. On alternate daily sessions, the mice were administered saline and confined to the other outer chamber. Mice received a total of 10 pairings during the conditioning phase (five with cocaine and five with saline). The side of the chamber assigned to cocaine administration was counterbalanced between mice. For the test phase (days 12–16), on the first test day, mice were allowed free access to the entire chamber for 20 min and time spent in each chamber was recorded for analysis of place conditioning. On the following four test days, mice received THIP or saline 20 min before testing and an injection of cocaine (10 mg/kg) or saline immediately before testing. Drugs were administered in a Latin square design and sessions were recorded for 20 minutes. THIP (or saline) was administered either intraperitoneally (8 mg/kg THIP) or intra-accumbally (0.5 μl; 3 mM THIP bilaterally), depending on the experiment.

Data analysis. CPP was calculated by subtracting the time spent in the cocaine-paired chamber with the time spent in the vehicle-paired chamber during the test phase (cocaine-saline time). CPP was tested using one-way repeated-measures ANOVA with preconditioning and post-conditioning cocaine-saline time as the dependent variables, and genotype as the between-subjects variable. THIP effects were analyzed separately with two two-way ANOVAs with cocaine-saline time for each infusion and injection as the dependent variables and genotype as the between-subjects variable. *Post hoc* comparisons were conducted using Tukey's test.

Drugs. Bicuculline methobromide (3×10^{-2} M), THIP (gaboxadol; 10^{-2} M), strychnine hydrochloride (10^{-3} M), SKF 81297 hydrobromide (10^{-2} M), R-(+)-SCH 23390 hydrochloride (10^{-2} M), (−)-quinpirole (10^{-2} M), and D-amphetamine sulfate (10^{-2} M) were prepared as aqueous stock solutions for subsequent dilution in ECS. Kynurenic acid (2×10^{-3} M) and GDPβS (5×10^{-4} M) were prepared directly into the extracellular and intracellular recording saline, respectively. DS2 (10^{-2} M) and (S)-(−)-sulpiride (2×10^{-3} M) were prepared as stock solutions in 100% DMSO. Drugs were obtained from Sigma-Aldrich or Tocris Bioscience with the exceptions of kynurenic acid (Ab-Cam Biochemicals) and cocaine hydrochloride (MacFarlan Smith). THIP and DS2 were kindly provided by Dr. Wafford (Merck). For behavioral experiments, both cocaine and THIP were dissolved in 0.9% saline and intraperitoneal injections were administered at a volume of 10 ml/kg.

Results
Cellular localization of the GABA$_A$R α4 and δ subunits in NAc
Immunohistochemistry and confocal microscopy determined the expression patterns of the GABA$_A$R α4 and δ subunits within the different cell types that comprise the NAc. Dopamine receptor phospho-protein 32 (DARPP-32), a cytosolic protein enriched in brain regions receiving dopaminergic input (Walaas and Greengard, 1984), was used to identify MSNs and to delineate the ventral striatum, which includes the NAc (Fig. 1). No apparent gradient in the intensity of the GABA$_A$R α4 and δ subunit immunoreactivity patterns was evident between the NAc core and shell subregions (Fig. 1), in agreement with previous reports exploring the mRNA and protein expression patterns of these two subunits in rats (Wisden et al., 1992; Pirker et al., 2000). Staining specificity was confirmed in GABA$_A$R subunit-specific gene-deleted α4$^{-/-}$ and $\delta^{-/-}$ mice (Fig. 1). The voltage-gated ion channel Kv2.1 and microtubule associated protein 2 (MAP-2) were used to visualize the MSN somatic plasma membrane and dendritic arbors, respectively. Both GABA$_A$R α4 and δ subunit immunoreactivity exhibited extensive colocalization with the membrane-bound signal of Kv2.1, whereas partial colocalization was evident with the cytoplasmically localized MAP-2 and DARPP-32 signal, confirming that these subunits are expressed on both somatic and dendritic surfaces of MSNs (Fig. 2A–C). Using BAC-transgenic mice (Gong et al., 2003) reporting either D1 or D2 receptors by the presence of green fluorescent protein (D1-EGFP or D2-EGFP, respectively), immunoreactivity for the GABA$_A$R α4 and δ subunits was consistently evident on both populations of MSNs, implying global expression of these proteins on these accumbal projection neurons (Fig. 2D). For MSNs, we found no evidence of GABA$_A$R δ subunit immunoreactivity colocalized with inhibitory synaptic markers such as gephyrin, the vesicular GABA transporter (VGAT), or neuroligin-2, suggesting a predominantly extrasynaptic location (Fig. 2E).

Neurochemical markers were used to determine whether identified interneurons (Kawaguchi et al., 1995) express GABA$_A$R α4 and δ subunits. Immunoreactivity for both subunits was evident on choline acetyl transferase (ChAT)-, parvalbumin (PV)-, and neuropeptide Y (NPY)-expressing neurons, but was not detected in somatostatin- and calretinin-expressing interneurons (Fig. 3).

α4$\beta\delta$ GABA$_A$Rs mediate a tonic conductance
For all NAc core MSNs, the GABA$_A$R antagonist bicuculline (30 μM; $V_h = -60$ mV, equal Cl$^-$$_i$/Cl$^-$$_o$) induced an outward, "tonic" current (24 $\pm$ 2.2 pA, $n = 32$) that was greatly reduced in equivalent neurons derived from either the $\delta^{-/-}$ (9 $\pm$ 1 pA, $n =$
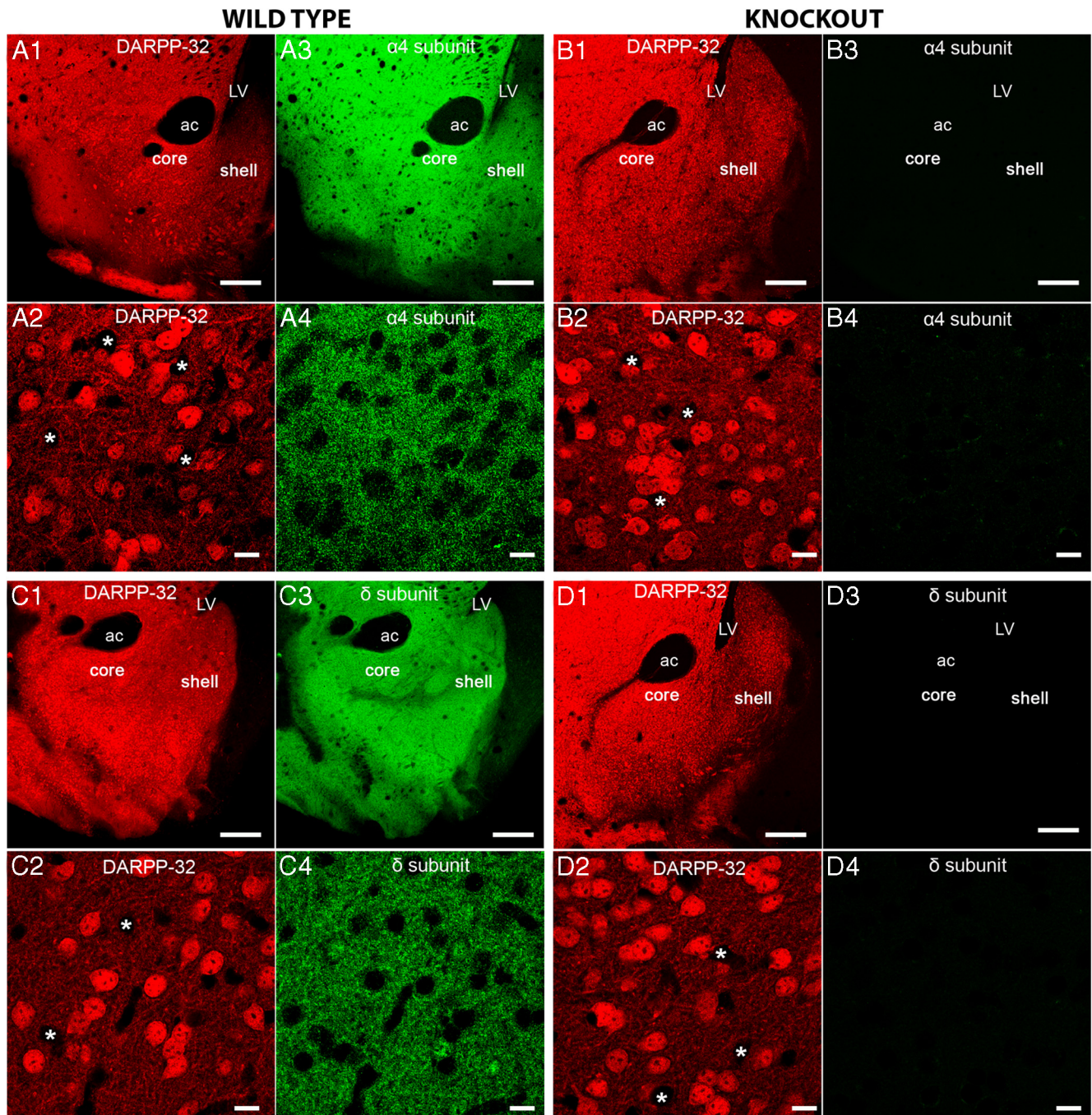
Figure 1. The distribution of GABA$_A$R α4 and δ subunit immunoreactivity in the ventral striatum closely overlaps with the distribution of medium spiny neurons (MSNs). **A**, **B**, Representative images of immunoreactivity for the GABA$_A$R α4 subunit and DARPP-32 in the ventral striatum, including the core and shell regions of the nucleus accumbens (NAc) in tissue from wild type (WT) and α4$^{-/-}$ mice, respectively. **A1** shows a regional overview and **A2** a magnified view of individual neurons expressing DARPP-32 immunoreactivity. DARPP-32 is only expressed in neurons that express dopamine receptors. Therefore, DARPP-32 immunoreactivity within the NAc is restricted to MSNs and not interneurons, which are likely to be those immunonegative neurons highlighted by the asterisks. **A3** and **A4** show the corresponding pattern of immunoreactivity for the GABA$_A$R α4 subunit in the regions represented in **A1** and **A2**. The GABA$_A$R α4 subunit signal closely correlates with that of DARPP-32 in the NAc, suggesting the widespread expression of the α4 subunit throughout the MSNs of this brain area. Furthermore, there is no discernible variation in the expression of the α4 subunit throughout the NAc subregions. **B1**, **B2**, There were no detectable differences in the immunoreactivity pattern of DARPP-32 in tissue from WT and α4$^{-/-}$ mouse, respectively. **B3**, **B4**, No specific GABA$_A$R α4 subunit signal was detected in tissue from GABA$_A$R α4$^{-/-}$ mice. **C1** shows a regional overview and **C2** a magnified view of individual neurons expressing DARPP-32 immunoreactivity. **C3** and **C4** show the corresponding pattern of immunoreactivity for the GABA$_A$R δ subunit in regions represented in **C1** and **C2**. Immunoreactivity for the GABA$_A$R δ subunit closely correlates with that of DARPP-32 in the NAc, suggesting widespread expression of the δ subunit throughout the MSNs of this brain area. Similar to the α4 subunit, there is no discernible variation in the expression of the δ subunit throughout the NAc. **D1**, **D2**, There were no detectable differences in the immunoreactivity pattern of DARPP-32 in tissue from WT and GABA$_A$R $\delta^{-/-}$ mice. **D3**, **D4**, No specific GABA$_A$R δ subunit signal was detected in tissue from GABA$_A$R $\delta^{-/-}$ mice. Scale bars: **A1**, **A3**, **B1**, **B3**, **C1**, **C3**, **D1**, **D3**, 300 μm; **A2**, **A4**, **B2**, **B4**, **C2**, **C4**, **D2**, **D4**, 10 μm. ac, Anterior commissure; LV, Lateral ventricle.

9; $t_{(39)} = 3.4$, $p < 0.01$, Student's unpaired t test) or the α4$^{-/-}$ (7 $\pm$ 2 pA, $n = 12$; $t_{(42)} = 4.4$, $p < 0.001$, Student's unpaired t test) mouse (Fig. 4A,D). In the dorsal striatum of immature mice, the tonic current is greater in D2- compared with D1-MSNs and is

primarily mediated by α5 subunit containing GABA$_A$Rs (Ade et al., 2008; Janssen et al., 2009; Santhakumar et al., 2010), whereas for mature mice, it is predominantly caused by δ-GABA$_A$Rs and is greater in D1- compared with D2-MSNs (Santhakumar et al.,
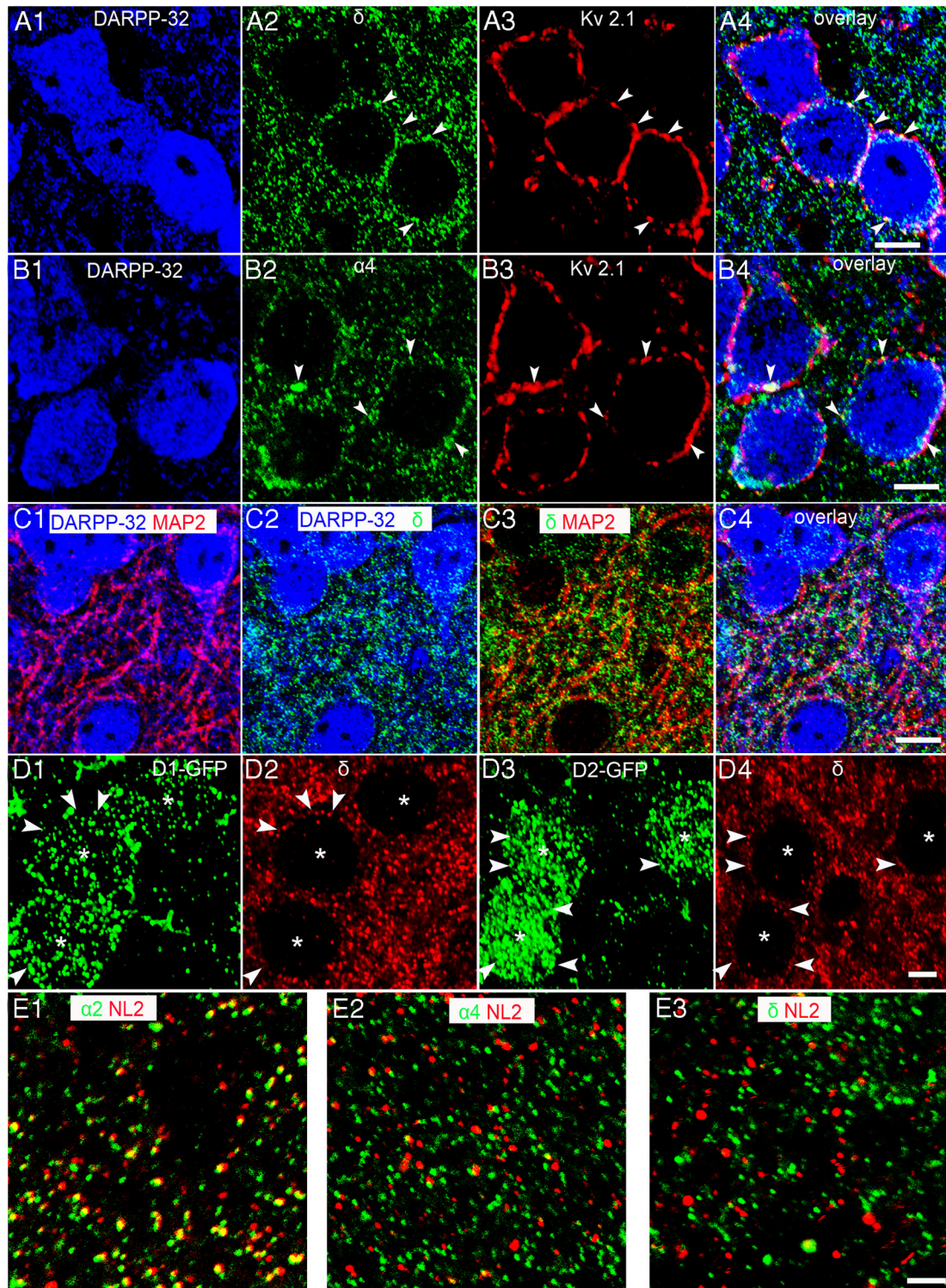
Figure 2. Cellular localization of the GABA$_A$R α4 and δ subunits in MSNs of the NAc core. *A1*,*B1*, DARPP-32 immunoreactivity is located within the cytoplasm of putative MSNs. *A2*, *B2*, Immunoreactivity for the GABA$_A$R δ and α4 subunits is clustered on both the somata (arrowheads) and dendritic profiles of DARPP-32-immunoreactive cells. *A3*, *B3*, Immunoreactivity for the voltage-gated potassium channel 2.1 (Kv2.1) delineates the somatic and proximal dendritic plasma membranes of putative MSNs. *A4*, *B4*, Overlay of *A1*–*A3* and *B1*–*B3* shows that GABA$_A$R δ and α4 subunit immunoreactive clusters, respectively, colocalize with that of Kv2.1 on DARPP-32-immunoreactive somata, confirming the clustering of the δ and the α4 subunit on the somatic plasma membranes of NAc MSNs. *C1*, DARPP-32-immunoreactive dendritic profiles colocalize with immunoreactivity for the dendritic marker MAP-2. *C2*, *C3*, Numerous GABA$_A$R δ subunit immunoreactive clusters are located on DARPP-32-immunoreactive dendritic profiles (*C2*) and on MAP-2 immunoreactive profiles (*C3*). *C4*, Overlay of *C1*–*C3* shows extensive clustering of GABA$_A$R δ subunit immunoreactivity on the dendrites of putative MSNs. *D1*, *D3*, Immunoreactivity for GFP in neurons (asterisks) of D1-EGFP and D2-EGFP mice, respectively. *D2*, *D4*, Immunoreactivity for the δ subunit is localized to somata (arrowheads) of both D1- and D2-EGFP-expressing cells, respectively, confirming the expression of this subunit in both subpopulations of MSNs. The expression pattern of the GABA$_A$R α4 subunit was indistinguishable from that of the GABA$_A$R δ subunit. *E1*, The majority of GABA$_A$R α2 subunit immunoreactive clusters colocalize with neuroligin-2 (NL2), a cell adhesion protein that is selectively expressed in inhibitory synapses. In contrast, the GABA$_A$R α4 subunit (*E2*) and GABA$_A$R δ subunit (*E3*) immunoreactive puncta are preferentially apposed to NL2 immunoreactive clusters, suggesting the subunit-specific targeting of GABA$_A$R subtypes to synaptic and extrasynaptic cell surfaces within the NAc. Scale bars: *A*, *B*, *D*, 5 μm; *C*, 10 μm; *E*, 2 μm.
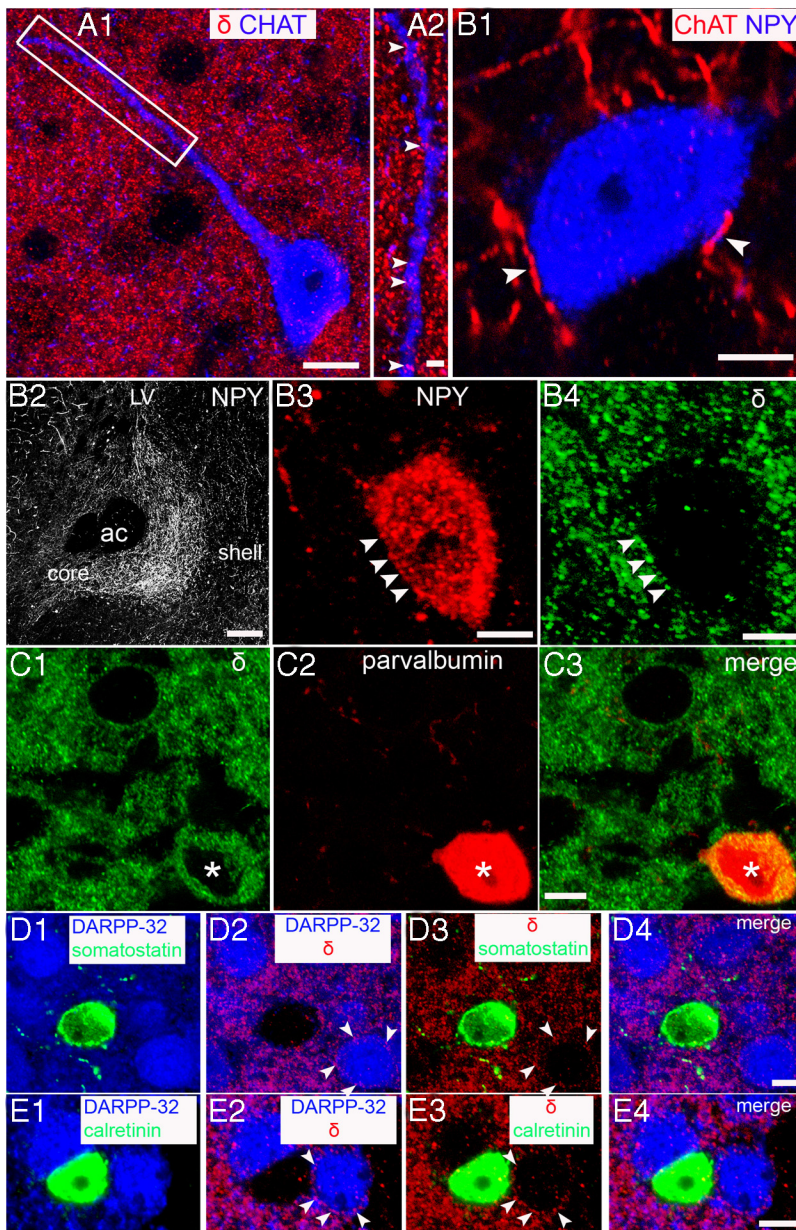
Figure 3. Cellular localization of the GABA$_A$R δ subunit in interneurons of the NAc. **A1**, Immunoreactivity for choline acetyltransferase (ChAT), a marker of cholinergic neurons, is evident in the neuronal soma and dendrites and in numerous varicosities throughout the field of view (FOV). Clustered immunoreactive signal for the GABA$_A$R δ subunit is consistent throughout the FOV, including the regions occupied by the ChAT-immunopositive neuron. **A2**, Magnified view of the boxed area in **A1** showing the numerous GABA$_A$R δ subunit-immunoreactive clusters (arrowheads) expressed on the ChAT-immunopositive dendrite. The expression pattern of the GABA$_A$R α4 subunit was indistinguishable from that of the GABA$_A$R δ subunit. **B**, Association of neuropeptide Y (NPY)-expressing neurons with ChAT and GABA$_A$R δ subunit immunoreactivity. **B1**, ChAT-immunoreactive axon terminals are closely associated (arrowheads) with an NPY-immunopositive neuron, suggesting cholinergic innervation of NPY interneurons. **B2**, Low-power overview of the expression of NPY within the NAc. Note the enrichment of NPY immunoreactivity within the core subregion of the NAc compared with the shell subregions. **B3**, An NPY-immunopositive neuron expressing GABA$_A$R δ subunit-immunoreactive clusters (**B4**, arrowheads) on the cell body. The expression pattern of the GABA$_A$R α4 subunit was indistinguishable from that of the GABA$_A$R δ subunit. **C1**, GABA$_A$R δ subunit immunoreactivity (asterisk) is expressed by a parvalbumin (PV)-expressing neuron (**C2**). **C3**, Overlay of **C1** and **C2**. Note that, compared with other neurons, which express the GABA$_A$R δ subunit on their somata, the signal in PV-expressing neurons is largely within the cytoplasm. The expression pattern of the GABA$_A$R α4 subunit was indistinguishable from that of the GABA$_A$R δ subunit. **D, E**, Immunoreactivity for the GABA$_A$R δ subunit is clearly distinguishable on putative MSNs (arrowheads). In contrast, no such signal was evident in somatostatin (**D**) or calretinin immunoreactive neurons (**E**), respectively. Scale bars: **A1**, 10 μm; **A2**, 2 μm; **B1**, 5 μm; **B2**, 200 μm; **B3** and **B4**, 5 μm; **C–E**, 5 μm.

2010). In the NAc core, staining for α4 and δ subunits was evident on both D1 and D2 neurons (Fig. 2) and functionally bicuculline (30 μM) produced a similar outward current for both D1-MSNs (41 ± 5 pA, $n = 15$) and D2-MSNs (30 ± 3 pA; $n = 11$; $t_{(24)} = 1.7$,

$p = 0.1$, Student's unpaired t test; Fig. 4D). Further evidence that both classes of MSNs express δ-GABA$_A$Rs is provided by the use of THIP and DS2 (see Results, Effect THIP and DS2 on MSNs). In contrast to the tonic current, the amplitude and kinetics of mIPSCs mediated by synaptic GABA$_A$Rs were not influenced by the deletion of the α4 or the δ subunit (Fig. 4B, Table 2).

Effect of THIP and DS2 on MSNs

The δ-GABA$_A$R selective agonist THIP (1 μM) induced an inward current ($-68 ± 8$ pA, $n = 8$) on all MSNs tested, an effect that was greatly reduced for equivalent neurons derived from either the δ$^{-/-}$ ($-14 ± 2$ pA, $n = 6$; $t_{(12)} = 5.9$, $p < 0.001$, Student's unpaired t test) or the α4$^{-/-}$ mouse ($-8 ± 3$ pA, $n = 9$; $t_{(15)} = 7.5$, $p < 0.001$, Student's unpaired t test; Fig. 4C–E). We demonstrated that DS2 acts as a selective positive allosteric modulator of δ-GABA$_A$Rs and thus enhances the tonic conductance of thalamocortical relay neurons of WT mice, but not of δ$^{-/-}$ mice (Wafford et al., 2009; Herd et al., 2013; Jensen et al., 2013). Similarly, DS2 (10 μM) induced an inward current for all WT MSNs ($-45 ± 7.8$ pA, $n = 9$), but not those derived from δ$^{-/-}$ ($-1.3 ± 0.6$ pA, $n = 6$; $t_{(13)} = 4.5$, $p < 0.001$, Student's unpaired t test) or α4$^{-/-}$ ($-1 ± 1.4$ pA, $n = 7$; $t_{(14)} = 4.8$, $p < 0.001$, Student's unpaired t test) mice (Fig. 4D,E). Regarding synaptic GABA$_A$Rs, DS2 (10 μM) had no significant effect on the mIPSC amplitude (control = $-70 ± 9$ pA; DS2 = $-73 ± 6$ pA; $n = 5$; $t_{(4)} = 0.18$, $p > 0.05$, Student's paired t test), rise time (control = $0.5 ± 0.1$ ms; DS2 = $0.5 ± 0.1$ ms; $n = 5$; $t_{(4)} = 2.16$, $p > 0.05$, Student's paired t test), or decay time (control = $7.7 ± 0.8$ ms; DS2 = $7.6 ± 0.7$; $n = 5$; $t_{(4)} = 0.15$, $p > 0.05$, Student's paired t test), although it did influence their frequency of occurrence (Fig. 5C).

Immunohistochemistry revealed staining for both the α4 and the δ subunit on particular interneurons (Fig. 3), suggesting that α4βδ receptors may also influence quantal GABA release onto accumbal MSNs. Consistent with this, THIP (1 μM) significantly decreased the frequency of both sIPSCs and mIPSCs ($t_{(7)} = 7.5$, $p = 0.001$ and $t_{(6)} = 3.77$, $p < 0.01$ respectively, Student's paired t test; Figure 5A,C). In contrast, THIP had no significant effect on the mIPSC frequency of MSNs derived from α4$^{-/-}$ or δ$^{-/-}$ mice ($t_{(8)} = 0.63$, $p > 0.05$, $t_{(5)} = 2.1$, $p > 0.05$, respectively, Student's paired t test; Figure 5B,C). Collectively, these data are consistent with the presence of α4βδ receptors on GABA-ergic interneurons innervating the
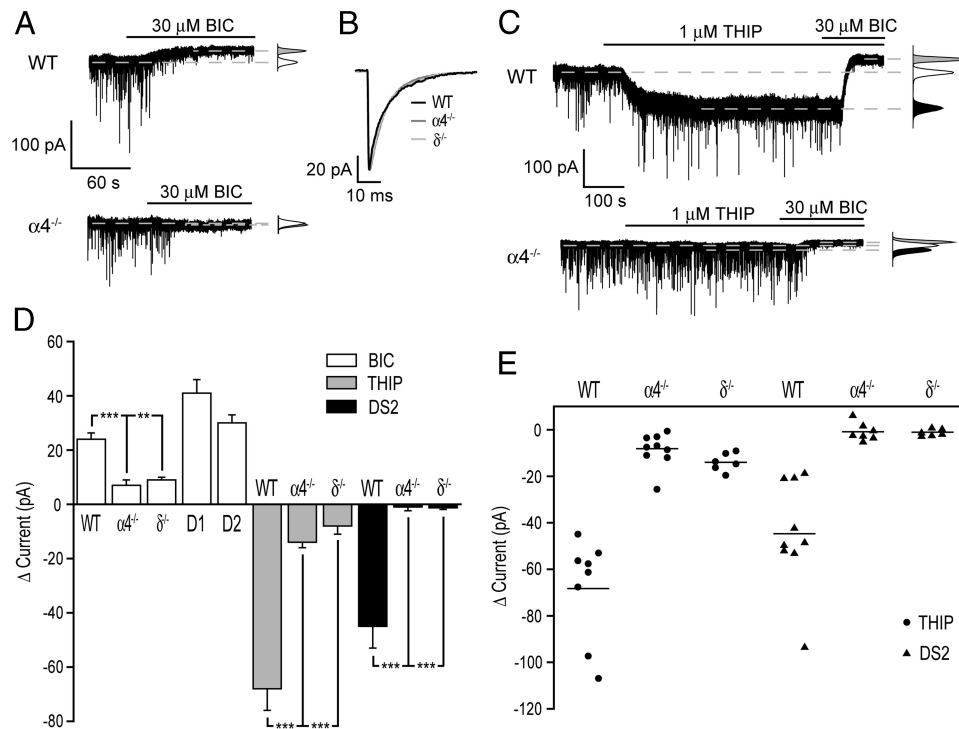
Figure 4. $\alpha4\beta\delta$ GABA$_A$Rs mediate a tonic current in NAc MSNs. **A**, Representative traces of whole-cell voltage-clamp recordings made from core MSNs derived from a WT and an $\alpha4^{-/-}$ mouse. The GABA$_A$R antagonist bicuculline (BIC 30 μM) produced an outward current and an associated decrease in membrane noise for the WT MSN, an effect greatly reduced for the equivalent recording from an $\alpha4^{-/-}$ MSN. The broken lines indicate the mean holding currents. The corresponding all-points histograms are given to the right of each trace (white = control, gray = + bicuculline). **B**, Illustrated are traces from representative MSNs giving the averaged superimposed mIPSCs recorded from neurons obtained from WT (black trace), $\alpha4^{-/-}$ (gray), and $\delta^{-/-}$ (light gray) mice, revealing that deletion of either of these subunits has no impact on the kinetics of the phasic currents mediated by synaptic receptors (note the amplitude is normalized to that of WT to aid a comparison of mIPSC time course). **C**, Representative traces illustrating that the selective δ-GABA$_A$R agonist THIP (1 μM) induces an inward current on a WT MSN, but has little effect on an equivalent neuron derived from an $\alpha4^{-/-}$ mouse. Note for the WT neuron that bicuculline (30 μM) reverses the THIP-induced inward current, but additionally induces an outward current (relative to the holding current before THIP), revealing again the presence of a tonic conductance cf. $\alpha4^{-/-}$ neurons. The broken lines indicate the mean holding current. The corresponding all-points histograms are given to the right of each trace [white = control; black = + THIP (1 μM); gray = THIP (1 μM) + bicuculline (30 μM)]. **D**, Histogram demonstrating that the mean outward current produced by bicuculline (30 μM; white columns) for WT neurons ($n = 32$) is greatly reduced for both $\alpha4^{-/-}$ ($n = 12$) and $\delta^{-/-}$ ($n = 9$) mice. Note that both D1- and D2-MSNs exhibit a tonic conductance as revealed by bicuculline (30 μM; white columns). Furthermore, the inward current produced by THIP (1 μM; gray columns) in WT neurons ($n = 8$), is greatly reduced for both $\alpha4^{-/-}$ ($n = 9$) and $\delta^{-/-}$ ($n = 6$) neurons. Similarly, DS2 (10 μM; black bars) produced an inward current in WT MSNs ($n = 9$), but was ineffective in equivalent recordings from $\alpha4^{-/-}$ ($n = 7$) or $\delta^{-/-}$ ($n = 6$) mice. The columns represent the mean $\pm$ SEM. $**p < 0.01$; $***p < 0.001$, Student's unpaired t tests. **E**, The scatter plot reveals that all MSNs obtained from WT mice exhibit a large inward current response to either THIP (1 μM) or to DS2 (10 μM) that was greatly reduced or absent in equivalent MSNs from $\alpha4^{-/-}$ or $\delta^{-/-}$ MSNs. The horizontal bar represents the mean. Collectively, these data suggest that all NAc core MSNs express functional $\alpha4\beta\delta$ GABA$_A$Rs.

**Table 2. The properties of mIPSCs recorded from NAc MSNs obtained from WT, $\alpha4^{-/-}$, and $\delta^{-/-}$ mice**

	WT	$\delta^{-/-}$	$\alpha4^{-/-}$
Peak amp (pA)	-87 ± 6 ($n = 31$)	-92 ± 9 ($n = 15$)	-75 ± 9 ($n = 12$)
Rise time (ms)	0.48 ± 0.01 ($n = 31$)	0.44 ± 0.02 ($n = 15$)	0.60 ± 0.02 ($n = 12$)
τw (ms)	8.7 ± 0.4 ($n = 31$)	8.1 ± 0.5 ($n = 15$)	9.0 ± 1.0 ($n = 12$)
Frequency (Hz)	1.5 ± 0.2 ($n = 36$)	2.6 ± 0.4 ($n = 19$)	1.7 ± 0.3 ($n = 17$)

MSNs, although, alternatively, the effect on GABA release may result from activation of these receptors on MSN axon collaterals (Koos et al., 2004; van Dongen et al., 2005; Taverna et al., 2008). The positive allosteric modulator DS2 also significantly reduced mIPSC and sIPSC frequency in WT MSNs ($t_{(6)} = 5.2, p < 0.01$ and $t_{(9)} = 3.7, p < 0.01$, respectively, Student's paired t test). The effect of DS2 on sIPSC frequency was further investigated for MSNs derived from $\alpha4^{-/-}$ or $\delta^{-/-}$ mice, in which it was inert ($t_{(7)} = 0.5, p > 0.05$ and $t_{(5)} = 0.17$, $p > 0.05$, respectively, Student's paired t test). Collectively, these findings suggest that in the presence of this drug, the levels of ambient GABA are sufficient to activate $\alpha4\beta\delta$ GABA$_A$Rs, which then influence quantal GABA release (Fig. 5C).

To elucidate the effects of THIP on the function of NAc MSNs, we initially performed gramicidin perforated-patch current-

clamp experiments to preserve the physiological intracellular Cl$^-$ concentration (Kyrozis and Reichling, 1995). Confirming previous reports (Bracci and Panzeri, 2006; Gerfen and Surmeier, 2011), NAc MSNs exhibited a relatively hyperpolarized RMP (-90 ± 1.9 mV, $n = 9$). Perforated-patch voltage-clamp experiments using focally applied GABA (1 mM) revealed an E_{GABA} of -72 ± 2 mV ($n = 9$). Therefore, we used an intracellular solution for current-clamp experiments containing a physiological [Cl$^-$] designed to mimic this reversal potential (calculated $E_{GABA} = -71$ mV). Input-output (I-O) experiments under these conditions revealed $\alpha4^{-/-}$ neurons to be more excitable than WT, with a leftward shift of the I-O relationship and a corresponding significant decrease of the rheobase (WT $= 125 \pm 10$ pA, $n = 22$; $\alpha4^{-/-} = 92 \pm 8$ pA, $n = 17$; $t_{(37)} = 6.2, p < 0.001$, Student's
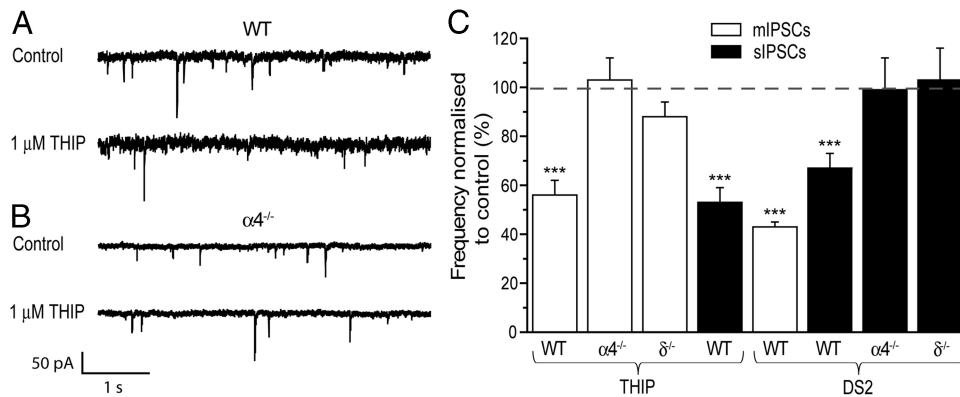
Figure 5. $\alpha4\beta\delta$ GABA$_A$Rs influence GABA release onto MSNs. Representative traces of paired recordings of mIPSCs obtained from WT (***A***, top two traces) and $\alpha4^{-/-}$ (***B***, bottom two traces) MSNs before and after THIP (1 μM). Note the decreased membrane noise associated with the $\alpha4^{-/-}$ compare with the WT recording due to the reduced tonic conductance in the former. ***C***, Histogram summarizing the effects of THIP (1 μM) expressed as a percentage of control, revealing this δ-selective agonist to produce a significant decrease in the mIPSC frequency of WT ($n = 7$), but not of $\alpha4^{-/-}$ ($n = 9$) or $\delta^{-/-}$ ($n = 6$) MSNs. THIP produced a similar reduction of the frequency of WT sIPSCs ($n = 8$). Similarly, DS2 (10 μM) decreased the frequency of mIPSCs ($n = 7$) and sIPSCs ($n = 10$) of WT MSNs, but not the sIPSC frequency of $\alpha4^{-/-}$ ($n = 8$) or $\delta^{-/-}$ ($n = 6$) MSNs. The bars (mIPSCs, white; sIPSCs, black) represent the mean $\pm$ SEM. ***$p < 0.001$ versus control by one-way repeated-measures ANOVA.

unpaired t test; Fig. 6). For WT MSNs, THIP (1 μM) reduced the number of action potentials elicited in response to current injection, causing a rightward shift of the I-O relationship (Fig. 6A) and a significant increase in the rheobase (139 $\pm$ 7% of control; $n = 9$; $F_{(1,8)} = 29.1$, $p < 0.001$, one-way repeated-measures ANOVA). Therefore, increasing the tonic current significantly reduced the excitability of accumbal MSNs. In contrast, for equivalent $\alpha4^{-/-}$ neurons, THIP (1 μM) had no effect on the I-O relationship (Fig. 6B) or on the rheobase (104 $\pm$ 5% of control; $F_{(1,6)} = 0.49$, $n = 7$; $p > 0.05$, one-way repeated-measures ANOVA).

Tonic current mediated by extrasynaptic $\alpha4\beta\delta$ receptors is selectively enhanced in D1-MSNs by the D1 agonist SKF81297 and by amphetamine

Given the importance of the dopaminergic innervation to NAc activity, we investigated whether the tonic current mediated by $\alpha4\beta\delta$ receptors was influenced by either D2 or D1 receptors. The acute application to D2-MSNs of either the D2 agonist quinpirole (10 μM, $n = 6$), or the D2 antagonist sulpiride (2 μM; $n = 6$) produced no change to the tonic current (Fig. 7A). However, prolonged exposure (>1 hour) to quinpirole (10 μM) produced a modest decrease of the tonic current of D2-MSNs, as revealed by the subsequent application of bicuculline (control = 30 $\pm$ 3 pA; $n = 11$; quinpirole = 20 $\pm$ 3 pA; $n = 6$; $t_{(15)} = 2.2$, $p < 0.05$, Student's unpaired t test; Fig. 7A).

The acute application of the D1 receptor agonist SKF81297 (10 μM) had no effect on D2-MSNs ($n = 4$), but for D1-MSNs, it induced an inward current ($\Delta I = -33 \pm 5$ pA, $n = 7$; Fig. 7A,B). The effect was G-protein coupled, because equivalent experiments performed with intracellular GDP-βS (0.5 mM) in the recording pipette greatly reduced the effect of SKF81297 (10 μM; $\Delta I = -10 \pm 4$ pA; $n = 6$; $t_{(11)} = 3.3$, $p < 0.01$, unpaired t test; Fig. 7A). The effect of the D1 agonist on the tonic current was well maintained because the application of bicuculline (30 μM) to D1-MSNs previously incubated in SKF81297 (10 μM) for >1 hour revealed a much greater outward current (100 $\pm$ 18 pA; $n = 6$) than equivalent control D1-MSNs (41 $\pm$ 5 pA; $n = 15$; $t_{(19)} = 4.3$, $p < 0.001$, Student's unpaired t test; Fig. 7A). In contrast to the D1 agonist, the acute application of the D1 antagonist SCH23390 (10 μM; $n = 4$) had no effect on the tonic current of D1-MSNs, suggesting that the ambient concentration of dopa-

mine in the slice was insufficient to influence the tonic current (Fig. 7A).

We next explored whether blocking the dopamine transporter by the psychostimulant cocaine would raise local extracellular dopamine to a level sufficient to influence the tonic conductance of D1-MSNs. However, using this *in vitro* paradigm, the bath application of cocaine (5 μM) had no effect on the tonic current ($\Delta I = -2 \pm 4$ pA; $n = 6$). In addition to blocking dopamine reuptake, amphetamine also causes displacement of this neurotransmitter from dopaminergic nerve terminals (Fleckenstein et al., 2007). Therefore, we investigated whether amphetamine might increase extracellular dopamine sufficiently to influence the tonic conductance of D1 neurons. In common with the D1 receptor agonist, application of amphetamine (10 μM) caused an inward current ($\Delta I = -26 \pm 5$ pA, $n = 7$) on D1-MSNs within a few minutes of being introduced to the slice (Fig. 7A). This effect of the psychostimulant was prevented by the coapplication of the D1 antagonist SCH23390 (10 μM; $\Delta I = -4 \pm 4$ pA, $n = 4$; $t_{(9)} = 2.9$, $p < 0.05$, Student's unpaired t test; Fig. 7A), demonstrating that amphetamine indirectly influences the GABA$_A$R-mediated tonic current of D1-MSNs by increasing the ambient dopamine concentration, which in turn activates D1 receptors.

Acute SKF81297 (10 μM) applied to D1-MSNs or quinpirole (10 μM) applied to D2-MSNs had no effect on the amplitude, kinetics, or frequency of mIPSCs mediated by synaptic GABA$_A$Rs (Table 3). Therefore, the dopamine receptor signaling pathway appears to selectively influence extrasynaptic, but not synaptic, GABA$_A$Rs.

$\alpha4\beta\delta$ receptors are involved in conditioned reward

Given the distribution of $\alpha4\beta\delta$ receptors on MSNs and their functional influence on neuronal excitability, we explored the consequences of deleting the $\alpha4$ subunit on the rewarding effects of psychostimulants through CPP. The ability of cocaine to support the formation of CPP (Fig. 8) was unaltered by a constitutive deletion of the $\alpha4$ subunit. Both WT and $\alpha4^{-/-}$ mice demonstrated an equal preference for the cocaine-paired chamber (Fig. 8A, main effect of conditioning: drug free, $F_{(1,20)} = 82.49$, $p < 0.001$; saline/saline test, $F_{(1,20)} = 12.70$, $p < 0.001$, and Fig. 8C, main effect of conditioning: drug free, $F_{(1,14)} = 41.53$, $p < 0.001$; saline/saline test, $F_{(1,14)} = 12.98$, $p < 0.001$). A challenge injection of cocaine (10 mg/kg, i.p.) given immediately before the prefer-
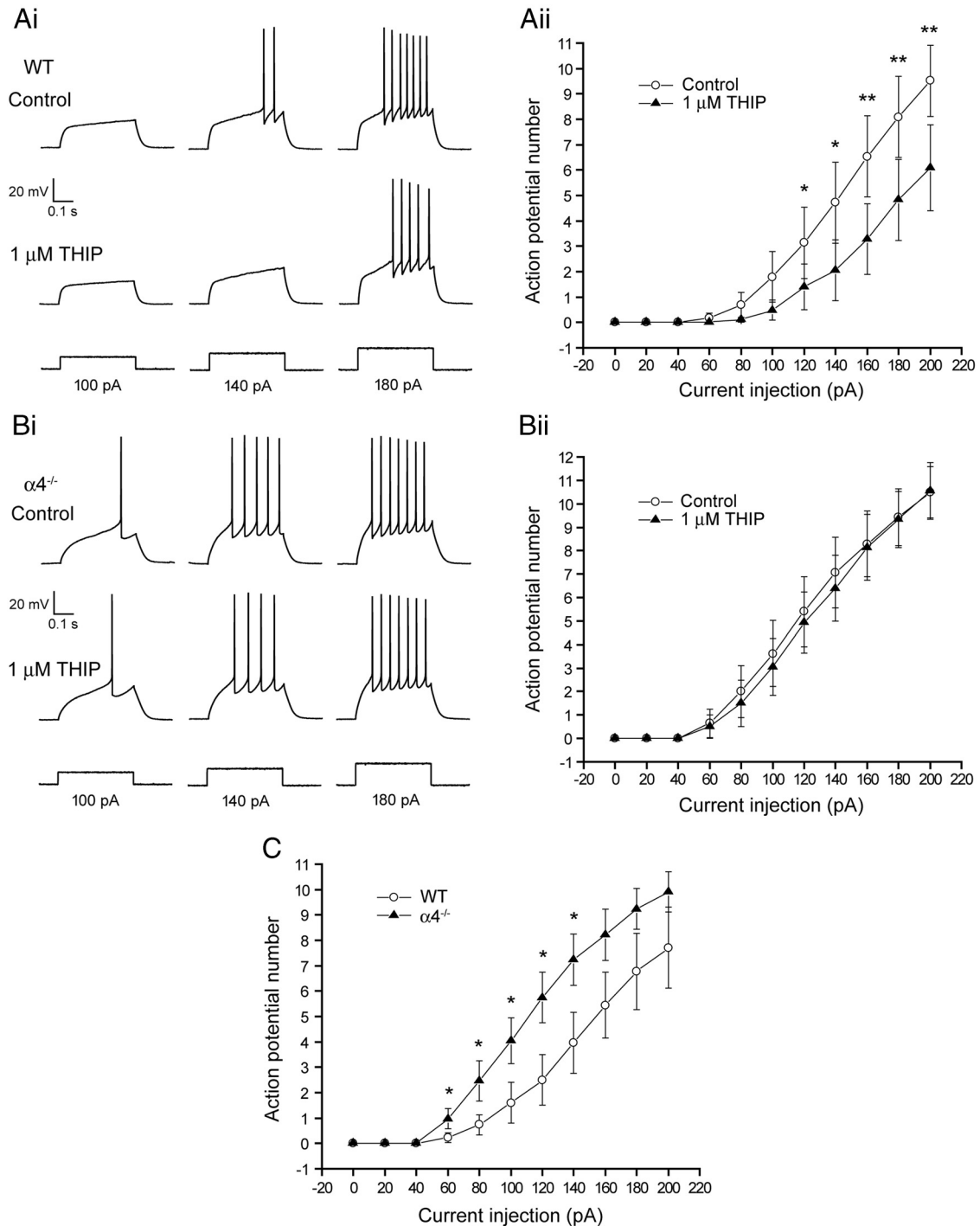
Figure 6. Deletion of the α4 subunit increases the excitability of accumbal MSNs and suppresses the inhibitory effect of THIP. *Ai*, *Bi*, Representative whole-cell current-clamp recordings of action potentials induced in response to current injection (100, 140, 180 pA; 400 ms duration) of MSNs from WT and α4$^{-/-}$ mice together with the associated input/output (I/O) curves. *Aii*, *Bii*, the number of action potentials discharged plotted as a function of the magnitude of the current injected examined over a greater range of current injections (20–200 pA, 20 pA increments). For all experiments, current injection was used to standardize the RMP of the MSN to −87 mV, a value similar to that determined from the gramicidin perforated-patch experiments (i.e., −90 mV). The intracellular solution for current-clamp experiments contained a physiological [Cl$^-$] designed to mimic the GABA reversal potential (calculated $E_{GABA} = -71$ mV) we obtained experimentally. Inspection of the representative control recordings in *A* and *B* reveals deletion of the α4 subunit, which decreases the tonic current to increase neuronal excitability in response to current injection. *C*, This feature is reinforced by the leftward shift of the I/O curve for MSNs derived from α4$^{-/-}$ mice (▲) compared with WT (○). Data were obtained from 17 and 22 MSNs, respectively (*$p < 0.05$; Student's unpaired t test). *Ai*, For WT MSNs, THIP (1 μM) increased the current required to elicit action potentials. *Aii*, The data obtained from nine paired cells (before and after THIP) is summarized as an I/O curve. For WT MSNs, the plot reveals THIP (▲) to cause a shift to the right of this relationship, indicating a reduced excitability compared with control (○; *$p < 0.05$; **$p < 0.01$ vs control by Student's paired t test). *Bi*, *Bii*, In contrast, THIP had no such effects on MSNs derived from α4$^{-/-}$ mice.

ence test significantly increased time in the cocaine-paired chamber compared with mice given saline (Fig. 8A, main effect of cocaine: $F_{(1,20)} = 18.65$, $p < 0.001$, and Fig. 8C, main effect of cocaine: $F_{(1,14)} = 15.38$, $p < 0.001$). To determine whether α4βδ

GABA$_A$Rs may influence this effect, systemic THIP (8 mg/kg, i.p.) was administered 20 min before CPP testing. There was no effect of THIP alone on the time spent in the cocaine-paired chamber, although THIP did block the cocaine enhancement of
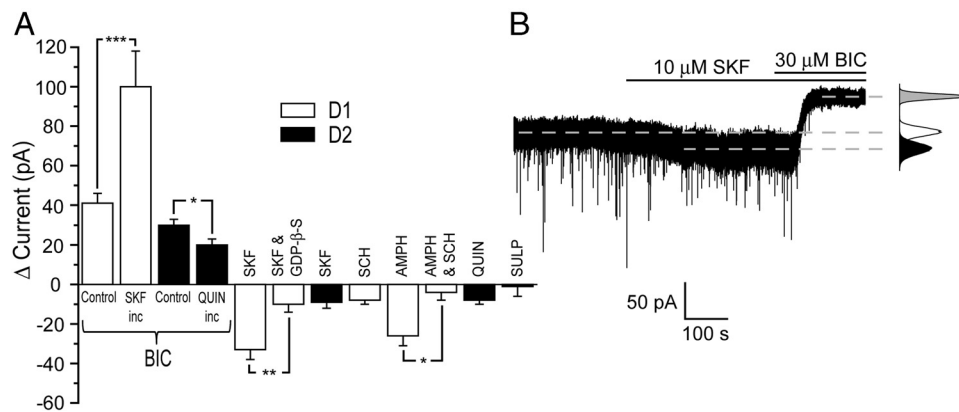
Figure 7. Influence of D1 and D2 receptor activation on the tonic current mediated by $\alpha4\beta\delta$ GABA$_A$Rs in D1-and D2-MSNs. **A**, Histogram illustrating the influence of D1 and D2 receptors on the tonic current mediated by $\alpha4\beta\delta$ GABA$_A$Rs expressed in D1-MSNs (white columns) and D2-MSNs (black columns). The acute application of the D1 antagonist SCH23390 (10 μM) had no effect on the tonic current of D1-MSNs. In contrast, the acute application of the D1 receptor agonist SKF81297 to D1-MSNs, but not to D2-MSNs, induced an inward current that was reduced by intracellular GDP-βS. Similarly, acute amphetamine (10 μM) induced an inward current for D1-MSNs. Note that the effect of amphetamine on D1-MSNs was prevented by the D1 antagonist SCH23390 (10 μM), demonstrating this psychostimulant to influence tonic inhibition by increasing ambient dopamine. The effect of D1 receptor activation on tonic inhibition is well maintained, because prolonged incubation (>1 hour) with SKF81297 caused a much greater tonic current (revealed by bicuculline 30 μM) in D1-MSNs compared with control. In contrast, D2 receptor activation by acute quinpirole (10 μM) and D2 receptor inhibition by acute sulpiride (2 μM) had no effect on the tonic current of D2-MSNs. However, prolonged incubation with quinpirole (10 μM) produced a modest decrease of the tonic current of D2-MSNs. The bars represent the mean ± SEM. *$p < 0.05$; **$p < 0.01$; ***$p < 0.001$, Student's unpaired t test. **B**, Representative trace demonstrating the increase in holding current produced by the bath application of SKF81297 (10 μM). Note that bicuculline (30 μM) reverses the increased current and reveals an additional outward current. The broken lines indicate the mean holding current. The corresponding all-points histograms are given to the right of the trace (white = control; black = + SKF81297; gray = SKF81297 + bicuculline). SKF, SKF81297; SULP, sulpiride; QUIN, quinpirole; SCH, SCH23390; AMPH, amphetamine; inc, incubated.

**Table 3. D1 and D2 receptor agonists do not influence the mIPSCs of D1- or D2-MSNs**

	D1-MSN control ($n = 6$)	D1-MSN 10 μM SKF81297 ($n = 6$)	D2-MSN control ($n = 5$)	D2-MSN 10 μM qunipirole ($n = 5$)
Peak amp (pA)	-80 ± 12	-71 ± 10	-64 ± 8	-63 ± 5
Rise time (ms)	0.54 ± 0.03	0.55 ± 0.03	0.55 ± 0.07	0.55 ± 0.06
τw (ms)	8.1 ± 0.4	8.1 ± 0.3	7.3 ± 0.6	7.9 ± 0.6
Frequency (Hz)	1.2 ± 0.5	1.1 ± 0.5	1.2 ± 0.5	1.3 ± 0.7

CPP, an effect completely absent in $\alpha4^{-/-}$ mice (Fig. 8A, genotype by cocaine by THIP interaction: $F_{(1,20)} = 12.40$, $p < 0.01$). To investigate whether accumbal $\alpha4\beta\delta$ GABA$_A$Rs mediate this suppressant effect of THIP, mice were cannulated and tested in the same paradigm. Intra-accumbal THIP had no effect on the expression of CPP, but, in common with the systemic dose, blocked cocaine-enhanced CPP in WT, but not $\alpha4^{-/-}$ mice (Fig. 8C, genotype by cocaine by THIP interaction: $F_{(1,14)} = 6.12$, $p < 0.05$). Therefore, we have revealed a role for accumbal $\alpha4\beta\delta$ GABA$_A$Rs in opposing the actions of cocaine on the enhancement of CPP.

Importantly, both D1- and D2-MSNs express functional $\alpha4\beta\delta$ GABA$_A$Rs, so simultaneous activation of these receptors on both cell populations might mask pathway-specific roles of tonic inhibition. Therefore, we tested CPP in mice with the $\alpha4$ subunit selectively deleted from cells expressing either D1 or D2 receptors, allowing us to dissociate roles that might be attributable to $\alpha4\beta\delta$ GABA$_A$Rs on one or other of the two MSN populations. The WT mice ("floxed $\alpha4$" mice) performed similarly to the WT mice in the previous experiments (compare Figs. 9, 8, respectively), confirming that the manipulations of the *gabra4* gene required to make the cell specific deletions were behaviorally silent (introduction of LoxP sites; Chandra et al., 2006). Importantly, CPP performance of the cell-specific knock-outs differed from the constitutive knock-outs. Mice with the $\alpha4$ subunit selectively ablated from D1-expressing neurons ($\alpha4^{D1-/-}$) showed greater CPP to cocaine (Fig. 9A, main effect of genotype: drug free, $F_{(1,18)} = 6.61$, $p < 0.05$, and saline/saline test, $F_{(1,18)} = 9.86$,

$p < 0.001$), whereas performance in the mice with the $\alpha4$ subunit selectively deleted from D2-containing neurons ($\alpha4^{D2-/-}$) was unaffected (Fig. 9C, main effect of conditioning: drug-free, $F_{(1,18)} = 54.35$, $p < 0.001$, and saline/saline test, $F_{(1,18)} = 43.73$, $p < 0.001$). As with the previous WT mice, a cocaine challenge during testing enhanced CPP in these WT mice (Fig. 9A, main effect of cocaine: $F_{(1,18)} = 22.44$, $p < 0.001$) and this effect could be blocked by the co-administration of THIP (8 mg/kg, i.p.). However, in common with the constitutive $\alpha4^{-/-}$ mice, the $\alpha4^{D1-/-}$ mice exhibited an enhancement of CPP by cocaine administered in the test phase that was not blocked by THIP (Fig. 9A, genotype by cocaine by THIP injection interaction, $F_{(1,18)} = 7.33$, $p < 0.01$). Although the $\alpha4^{D2-/-}$ mice showed similar cocaine CPP performance to WTs (Fig. 9C), they showed no cocaine enhancement of CPP (Fig. 9C, cocaine by genotype interaction, $F_{(1,18)} = 18.31$, $p < 0.001$). Finally, THIP had no effect alone on expression of CPP in any genotype and no effect in combination with cocaine in the $\alpha4^{D2-/-}$ mice (Fig. 9C, genotype by cocaine by THIP injection interaction, $F_{(1,18)} = 9.12$, $p < 0.01$).

Locomotor activity was measured during the CPP testing sessions (Figs. 8B,D, 9B,D). No differences in locomotor activity were observed across genotypes or with THIP administration. Cocaine increased activity across genotypes and conditions (main effect of cocaine, Fig. 8B: $F_{(1,20)} = 96.28$, $p < 0.001$, 8D: $F_{(1,14)} = 68.02$, $p < 0.001$, 9B, $F_{(1,18)} = 77.56$, $p < 0.001$) 9D $F_{(1,18)} = 88.50$, $p < 0.001$) and this increase was unaffected by THIP.
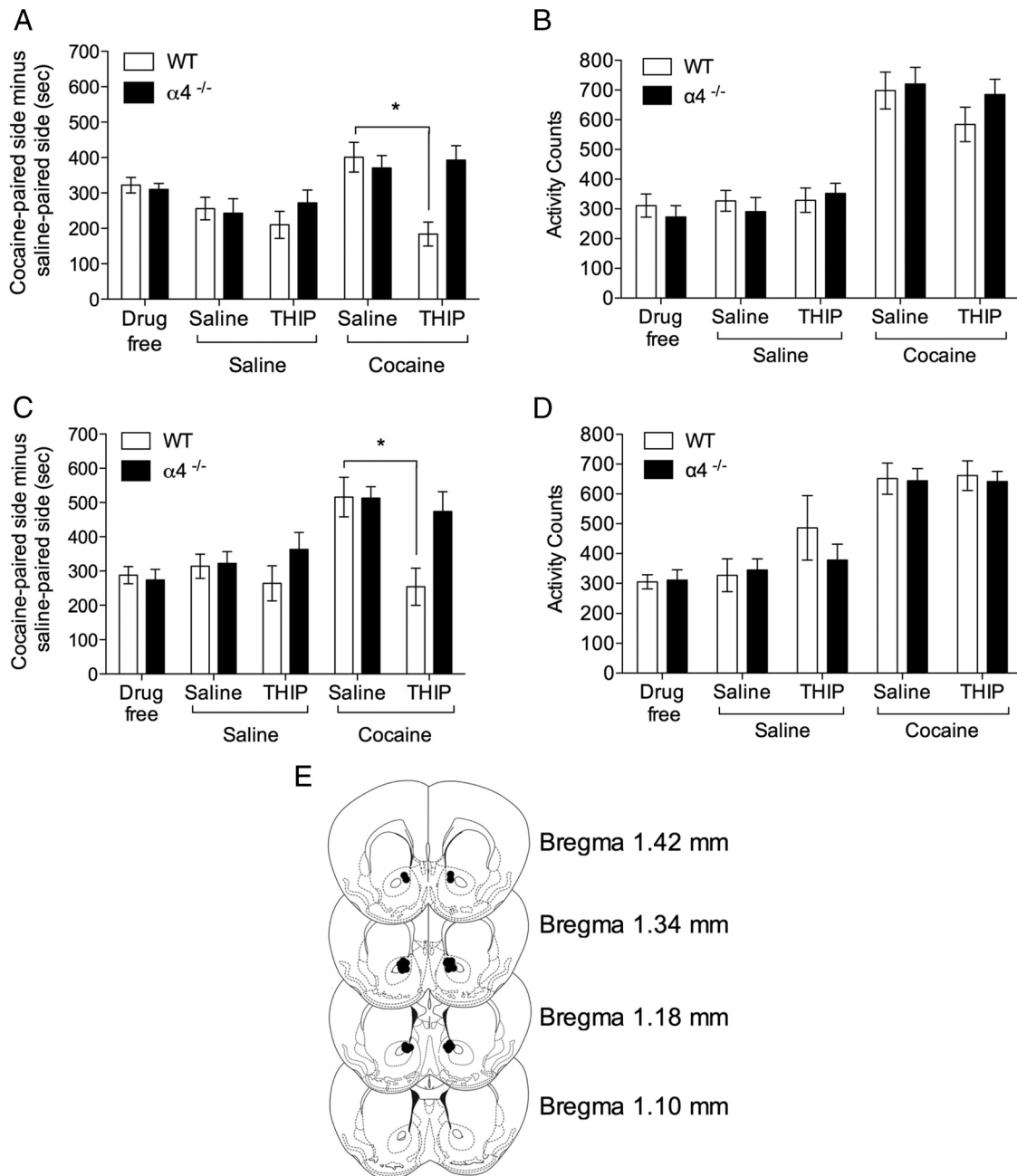
Figure 8. Conditioned place preference (CPP) and locomotor activity in $\alpha 4$ constitutive knock-out mice. **A**, Cocaine induced a significant CPP in both WT ($n = 11$) and constitutive $\alpha 4^{-/-}$ ($n = 11$) mice under drug-free and saline (saline/saline) conditions. Systemic THIP had no effect on preference in either genotype (THIP/saline). A challenge dose of cocaine increased preference in both genotypes (saline/cocaine) and THIP blocked the cocaine enhancement in WT, but not $\alpha 4^{-/-}$ mice (THIP/cocaine). **B**, WT and $\alpha 4^{-/-}$ mice did not significantly differ in locomotor activity during CPP testing and activity was potentiated by a cocaine challenge in both genotypes. Systemic THIP (8 mg/kg) did not alter activity during testing in either genotype. **C**, As in **A**, cocaine induced a significant CPP in both WT ($n = 8$) and constitutive $\alpha 4^{-/-}$ ($n = 8$) mice under drug-free and saline conditions. Intra-accumbal THIP had no effect on preference in either genotype. Again, a challenge dose of cocaine enhanced preference in both genotypes. This effect was blocked by intra-accumbal THIP in WT, but not in $\alpha 4^{-/-}$ mice. **D**, As in **B**, WT and $\alpha 4^{-/-}$ mice did not significantly differ in locomotor activity during CPP testing and were both equally potentiated by a cocaine challenge. Intra-accumbal infusion of 3 mM THIP did not alter activity during testing in either genotype. **E**, Cannulae placements for intra-accumbal infusion in **C** and **D**. *$p < 0.05$, post hoc comparisons.

Discussion

Previous studies of $GABA_AR$-mediated inhibition in the NAc have focused on synaptic receptors (Morris et al., 2008; Dixon et al., 2010); however, reducing NAc $\alpha 4$ or δ subunit expression also alters drug taking (Nie et al., 2011; Rewal et al., 2012). In thalamus and hippocampus, $\alpha 4 \beta \delta$-$GABA_ARs$ are expressed peri- or extrasynaptically and mediate a tonic conductance (Belelli et al., 2005; Farrant and Nusser, 2005; Brickley and Mody, 2012; Herd et al., 2013; Wlodarczyk et al., 2013). In the NAc, $\alpha 4$ and δ subunit staining was evident in the core and shell regions of the cell body and dendrites of both D1- and D2-MSNs. Functionally, a tonic current was evident for both D1- and D2-MSNs, which was greatly reduced by deletion of the $\alpha 4$ or the δ subunit, manipulations that had no effect on the properties of mIPSCs mediated by synaptic $GABA_ARs$. Consistent with this, in MSNs, $\alpha 4$ or δ subunit staining showed limited or no colocalization, respec-
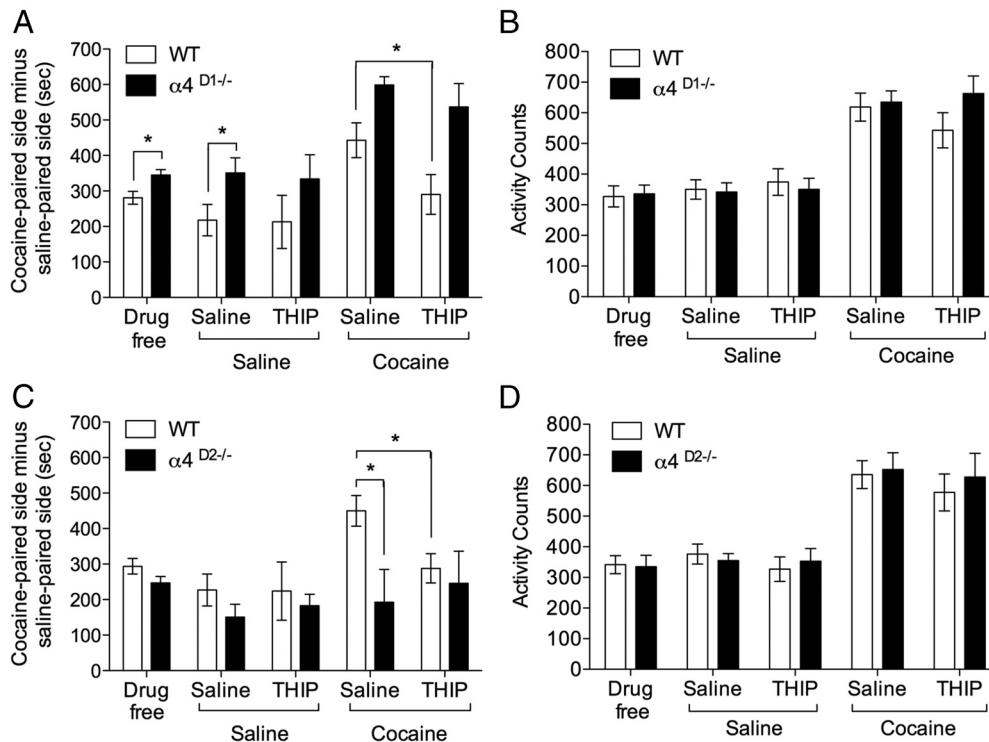
Figure 9. CPP and locomotor activity in $\alpha 4$ cell-specific knock-out mice. ***A***, Mice with $\alpha 4$ selectively ablated from D1-expressing neurons ($\alpha 4^{D1-/-}$, $n = 10$) showed greater cocaine-induced CPP than WTs ($n = 10$). Systemic THIP had no effect on preference in either genotype (THIP/saline). A challenge dose of cocaine enhanced preference in both genotypes (saline/cocaine) and THIP blocked this enhancement in WT, but not $\alpha 4^{D1-/-}$ mice (THIP/cocaine). ***B***, WT and $\alpha 4^{D1-/-}$ mice did not significantly differ in locomotor activity during CPP and activity was potentiated by a cocaine challenge in both genotypes. THIP (8 mg/kg, i.p.) did not alter activity during testing in either genotype. ***C***, Cocaine induced CPP in both WT ($n = 10$) and mice with $\alpha 4$ selectively ablated from D2-expressing neurons ($\alpha 4^{D2-/-}$, $n = 10$). However, the cocaine enhancement of preference seen in WT was not present in $\alpha 4^{D2-/-}$ mice (saline/cocaine). THIP blocked the cocaine enhancement in WT, but had no effect on performance in $\alpha 4^{D2-/-}$ mice (THIP/cocaine). ***D***, Locomotor activity did not differ between WT and $\alpha 4^{D2-/-}$ mice during CPP and activity was potentiated by a cocaine challenge in both genotypes. THIP (8 mg/kg, i.p.) did not alter activity during testing in either genotype. $*p < 0.05$, post hoc comparisons.

tively, with the synaptic markers gephyrin, VGAT, or neuroligin-2. Both the δ-GABA$_A$R-selective PAM DS2 and the selective agonist THIP, induced a large inward current for all MSNs, that was negated or substantially reduced for equivalent recordings from $\delta^{-/-}$ or $\alpha 4^{-/-}$ neurons, further supporting the expression of these receptors in both D1- and D2-MSNs. Functionally, THIP decreased MSN excitability in WT mice, but not $\alpha 4^{-/-}$ mice, whereas $\alpha 4$ subunit deletion increased basal excitability.

Staining for $\alpha 4$ and δ subunits was additionally evident in PV-, ChAT-, and NPY-expressing interneurons. In ChAT and NPY interneurons, expression was primarily restricted to dendritic or somatic plasma membranes, respectively. In contrast, for PV-expressing interneurons, immunoreactivity was primarily cytoplasmic, suggesting that $\alpha 4 \beta \delta$-GABA$_A$Rs in these neurons may be targeted to cell surfaces other than those on somata and dendrites (e.g., presynaptic terminals). The location of interneuronal $\alpha 4 \beta \delta$ GABA$_A$Rs suggests that, in common with VTA interneurons, they influence neurotransmitter release (Xiao et al., 2007; Vashchinkina et al., 2012). Indeed, THIP reduced the frequency of mIPSCs and sIPSCs of WT, but not $\delta^{-/-}$ or $\alpha 4^{-/-}$ MSNs. However, such effects could reflect receptor activity located on axon collaterals forming synapses on the MSNs (Koos et al., 2004; van Dongen et al., 2005; Taverna et al., 2008). DS2 also reduced sIPSC frequency of WT, but not of $\alpha 4^{-/-}$ or $\delta^{-/-}$ MSNs. Because DS2 is an allosteric modulator, this suggests that, in the presence of the drug, ambient GABA concentrations are sufficient to activate these upstream $\alpha 4 \beta \delta$ GABA$_A$Rs and influence GABA release.

A role for these receptors in opposing cocaine's effects was revealed by a THIP-induced reduction of cocaine-enhanced CPP in WT, but not constitutive $\alpha 4^{-/-}$ mice. The systemic effects of THIP are complex, because it will activate other δ-GABA$_A$Rs (e.g., in thalamus, hippocampus, VTA) and at high doses may engage additional GABA$_A$R isoforms (Mortensen et al., 2010). Nevertheless, in this study, the sedative effects of THIP given intraperitoneally (Herd et al., 2009; Vashchinkina et al., 2012) should not affect CPP performance. First, THIP was administered 20 minutes before the CPP test, and under these conditions, we did not detect an effect of THIP on locomotor activity during the CPP experiment. Second, locomotor activity can be inversely proportional to CPP magnitude (Gremel and Cunningham, 2007), so a small sedative effect of systemic THIP might be expected to increase CPP. Here, THIP either had no effect or reduced CPP. We therefore attribute its actions to a direct effect on CPP. This effect of systemic THIP was specific, because the suppression of cocaine CPP was evident in WT, but not in $\alpha 4^{-/-}$ mice. Importantly, infusion of THIP directly into the NAc was equally effective at blocking the cocaine enhancement of CPP in WT, but not $\alpha 4^{-/-}$ mice, revealing that, in this behavior, accumbal $\alpha 4 \beta \delta$ GABA$_A$Rs are the principal site of action of systemic THIP.

Our electrophysiological studies revealed the actions of THIP in the NAc to be complex, influencing GABA release and activating extrasynaptic receptors of MSNs. Functionally, the predominant effect of THIP is probably a suppression of MSN excitability due to activation of extrasynaptic $\alpha 4 \beta \delta$ receptors on the MSN causing an associated decreased input resistance.

However, because δ-GABA$_A$Rs are expressed on both D1- and D2-MSNs, THIP will decrease the ability of excitatory inputs to generate an action potential in the MSN output projections of both the indirect and direct pathways. Because these MSN subtypes can exert opposing actions on certain psychostimulant-induced behaviors (Hikida et al., 2010; Lobo et al., 2010; Beutler et al., 2011; Ferguson et al., 2011), tonic inhibition via α4βδ-GABA$_A$Rs might cause quite different effects via these two output pathways. To probe pathway-specific effects of α4βδ-GABA$_A$Rs, we investigated cocaine CPP in mice with the α4 subunit ablated specifically from either D1- or D2-expressing neurons. Although this strategy also targets other D1- or D2-expressing neuronal populations (e.g., cortex, dorsal striatum), our experiments using THIP administered into NAc strongly implicate accumbal α4βδ-GABA$_A$Rs in cocaine's ability to enhance CPP, thus allowing a potential dissociation of the roles of α4βδ-GABA$_A$Rs on D1 or D2-MSN output pathways of the striatum. Deleting the α4 subunit from D1-neurons facilitated conditioning, as evidenced by more time spent in the cocaine-paired chamber during the test phase. This result agrees with a classic model of striatal processing, suggesting that activation of the direct pathway is rewarding (Kravitz and Kreitzer, 2012). Optogenetic stimulation of the direct pathway neurons in the NAc during training enhances cocaine-CPP (Lobo et al., 2010). Here, by decreasing tonic GABAergic inhibition and thereby increasing D1-MSN excitability, mice similarly showed greater cocaine-CPP.

Dopamine actions on D1-MSNs are complex, causing both excitatory and opposing inhibitory effects on the activity of various receptors and ion channels (Gerfen and Surmeier, 2011). Now adding further complexity, we demonstrate that the GABAergic tonic current in D1-MSNs is dynamically increased by D1 receptor activation, achieved directly by a selective agonist, or indirectly by amphetamine, thereby limiting excitatory effects of dopamine. The enhanced tonic current was prevented by blocking G-protein coupling by intracellular GDP-βs and therefore was unlikely to be caused indirectly (e.g., modifying GABA release), but occurred within the D1-MSN. In contrast, prolonged, but not acute, D2 receptor activation caused a modest decrease of the tonic conductance of D2-MSNs. A similar differential effect of dopamine receptor activation on the tonic conductance of D1- and D2-MSNs occurs in the dorsal striatum, reflecting the distinct effects of these receptors on protein kinase A (Janssen et al., 2009).

Behaviorally, the role of tonic inhibition was revealed by deletion of the α4 subunit selectively from D1- and D2-expressing neurons. The D1 neuron deletion enhanced cocaine-CPP, presumably reflecting an increase in D1-MSN excitability. Therefore, D1-MSN α4βδ-GABA$_A$Rs may act as an immediate homeostatic control to prevent excessive neuronal excitation by dopamine. Interestingly, chronic cocaine induced an upregulation of the *gabra4* gene specifically in D1-MSNs (Heiman et al., 2008), suggesting that in addition to providing a short-term homeostatic role when excessively stimulated by dopamine, expression of α4βδ-GABA$_A$Rs may be increased, thereby strengthening an inhibitory "brake" on D1-MSNs. The cocaine enhancement of CPP is unlikely to be due to the locomotor-activating properties of the drug, because increased activity might interfere with the expression of CPP (Gremel and Cunningham, 2007). Instead, the interoceptive properties of cocaine may be increasing the salience of the CPP context and consequently increasing the expression of conditioned reward (Cunningham and Noble, 1992; Bespalov et al., 1999). This acute cocaine effect was blocked in WT mice by

intra-accumbal THIP and is presumably mediated by α4βδ-GABA$_A$Rs on D1-expressing neurons, because the agonist is inert in both constitutive α4$^{-/-}$ mice and in α4$^{D1-/-}$ mice. Interestingly, in α4$^{D2-/-}$ mice, the cocaine enhancement of CPP is absent. *In vitro*, prolonged, but not acute, D2 receptor activation produced a modest decrease of the D2-MSN tonic current, presumably thereby increasing D2-MSN excitability. The deletion of the α4 subunit will further increase the likelihood of firing in these D2-MSNs. That THIP did not decrease CPP in the absence of cocaine suggests that this increase in firing is expressed only when there is a robust increase in synaptic dopamine, such as that which occurs with psychostimulants. With regard to the cocaine enhancement of CPP, ablation of α4βδ-GABA$_A$Rs from D1 neurons may predominate in the phenotype of constitutive α4$^{-/-}$, because the α4$^{D1-/-}$ mice show the same phenotype. Therefore, either the D2-neuron α4βδ-GABA$_A$R effect on cocaine enhancement of preference is upstream of the D1 effect or the effects on the direct pathway simply dominate those of the indirect pathway in the constitutive knock-out. Collectively, these data suggest that the major role of α4βδ-GABA$_A$Rs in controlling CPP performance is the regulation of D1-MSN firing.

In conclusion, α4βδ GABA$_A$Rs expressed on NAc D1-MSNs mediate tonic inhibition that is enhanced by a D1 receptor agonist or by amphetamine. Behaviorally, accumbal activation of these receptors opposes cocaine enhancement of CPP and their absence from D1-expressing neurons enhances cocaine-CPP. We speculate that α4βδ GABA$_A$Rs of D1-MSNs act to limit the overall excitatory actions of dopamine by providing an inhibitory "brake." Collectively, these studies identify α4βδ GABA$_A$Rs as a potential therapeutic target for influencing addictive behaviors.

References

Ade KK, Janssen MJ, Ortinski PI, Vicini S (2008) Differential tonic GABA conductances in striatal medium spiny neurons. J Neurosci 28:1185–1197. CrossRef Medline

Belelli D, Peden DR, Rosahl TW, Wafford KA, Lambert JJ (2005) Extrasynaptic GABA$_A$ receptors of thalamocortical neurons: a molecular target for hypnotics. J Neurosci 25:11513–11520. CrossRef Medline

Bespalov AY, Tokarz ME, Bowen SE, Balster RL, Beardsley PM (1999) Effects of test conditions on the outcome of place conditioning with morphine and naltrexone in mice. Psychopharmacology (Berl) 141:118–122. CrossRef Medline

Beutler LR, Wanat MJ, Quintana A, Sanz E, Bamford NS, Zweifel LS, Palmiter RD (2011) Balanced NMDA receptor activity in dopamine D1 receptor (D1R)- and D2R-expressing medium spiny neurons is required for amphetamine sensitization. Proc Natl Acad Sci U S A 108:4206–4211. CrossRef Medline

Bracci E, Panzeri S (2006) Excitatory GABAergic effects in striatal projection neurons. J Neurophysiol 95:1285–1290. Medline

Brickley SG, Mody I (2012) Extrasynaptic GABA$_A$ receptors: their function in the CNS and implications for disease. Neuron 73:23–34. CrossRef Medline

Chandra D, Jia F, Liang J, Peng Z, Suryanarayanan A, Werner DF, Spigelman I, Houser CR, Olsen RW, Harrison NL, Homanics GE (2006) GABA$_A$ receptor α4 subunits mediate extrasynaptic inhibition in thalamus and dentate gyrus and the action of gaboxadol. Proc Natl Acad Sci U S A 103:15230–15235. CrossRef Medline

Corteen NL, Cole TM, Sarna A, Sieghart W, Swinny JD (2011) Localization of GABA$_A$ receptor α subunits on neurochemically distinct cell types in the rat locus coeruleus. Eur J Neurosci 34:250–262. CrossRef Medline

Cunningham CL, Noble D (1992) Methamphetamine-induced conditioned place preference or aversion depending on dose and presence of drug. Ann N Y Acad Sci 654:431–433. CrossRef Medline

Dixon CI, Morris HV, Breen G, Desrivieres S, Jugurnauth S, Steiner RC, Vallada H, Guindalini C, Laranjeira R, Messas G, Rosahl TW, Atack JR, Peden DR, Belelli D, Lambert JJ, King SL, Schumann G, Stephens DN (2010) Cocaine effects on mouse incentive-learning and human addiction are linked to $\alpha2$ subunit-containing $GABA_A$ receptors. Proc Natl Acad Sci U S A 107:2289–2294. CrossRef Medline

Dugué GP, Dumoulin A, Triller A, Dieudonne S (2005) Target-dependent use of co-released inhibitory transmitters at central synapses. J Neurosci 25:6490–6498. CrossRef Medline

Everitt BJ, Dickinson A, Robbins TW (2001) The neuropsychological basis of addictive behaviour. Brain Res Brain Res Rev 36:129–138. CrossRef Medline

Farrant M, Nusser Z (2005) Variations on an inhibitory theme: phasic and tonic activation of $GABA_A$ receptors. Nat Rev Neurosci 6:215–229. CrossRef Medline

Ferguson SM, Eskenazi D, Ishikawa M, Wanat MJ, Phillips PE, Dong Y, Roth BL, Neumaier JF (2011) Transient neuronal inhibition reveals opposing roles of indirect and direct pathways in sensitization. Nat Neurosci 14:22–24. CrossRef Medline

Fleckenstein AE, Volz TJ, Riddle EL, Gibb JW, Hanson GR (2007) New insights into the mechanism of action of amphetamines. Annu Rev Pharmacol Toxicol 47:681–698. CrossRef Medline

Gerfen CR, Surmeier DJ (2011) Modulation of striatal projection systems by dopamine. Annu Rev Neurosci 34:441–466. CrossRef Medline

Gerfen CR, Engber TM, Mahan LC, Susel Z, Chase TN, Monsma FJ Jr, Sibley DR (1990) D1 and D2 dopamine receptor-regulated gene expression of striatonigral and striatopallidal neurons. Science 250:1429–1432. CrossRef Medline

Gong S, Zheng C, Doughty ML, Losos K, Didkovsky N, Schambra UB, Nowak NJ, Joyner A, Leblanc G, Hatten ME, Heintz N (2003) A gene expression atlas of the central nervous system based on bacterial artificial chromosomes. Nature 425:917–925. CrossRef Medline

Gong S, Doughty M, Harbaugh CR, Cummins A, Hatten ME, Heintz N, Gerfen CR (2007) Targeting Cre recombinase to specific neuron populations with bacterial artificial chromosome constructs. J Neurosci 27:9817–9823. CrossRef Medline

Gremel CM, Cunningham CL (2007) Role of test activity in ethanol-induced disruption of place preference expression in mice. Psychopharmacology (Berl) 191:195–202. CrossRef Medline

Heiman M, Schaefer A, Gong S, Peterson JD, Day M, Ramsey KE, Suárez-Fariñas M, Schwarz C, Stephan DA, Surmeier DJ, Greengard P, Heintz N (2008) A translational profiling approach for the molecular characterization of CNS cell types. Cell 135:738–748. CrossRef Medline

Herd MB, Foister N, Chandra D, Peden DR, Homanics GE, Brown VJ, Balfour DJ, Lambert JJ, Belelli D (2009) Inhibition of thalamic excitability by 4,5,6,7-tetrahydroisoxazolo[4,5-c]pyridine-3-ol: a selective role for δ-$GABA_A$ receptors. Eur J Neurosci 29:1177–1187. CrossRef Medline

Herd MB, Brown AR, Lambert JJ, Belelli D (2013) Extrasynaptic $GABA_A$ receptors couple presynaptic activity to postsynaptic inhibition in somatosensory thalamus. J Neurosci 33:14850–14868. CrossRef Medline

Hikida T, Kimura K, Wada N, Funabiki K, Nakanishi S (2010) Distinct roles of synaptic transmission in direct and indirect striatal pathways to reward and aversive behavior. Neuron 66:896–907. CrossRef Medline

Janssen MJ, Ade KK, Fu Z, Vicini S (2009) Dopamine modulation of GABA tonic conductance in striatal output neurons. J Neurosci 29:5116–5126. CrossRef Medline

Jensen ML, Wafford KA, Brown AR, Belelli D, Lambert JJ, Mirza NR (2013) A study of subunit selectivity, mechanism and site of action of the δ selective compound 2 (DS2) at human recombinant and rodent native $GABA_A$ receptors. Br J Pharmacol 168:1118–1132. CrossRef Medline

Kawaguchi Y, Wilson CJ, Augood SJ, Emson PC (1995) Striatal interneurones: chemical, physiological and morphological characterization. Trends Neurosci 18:527–535. CrossRef Medline

Koos T, Tepper JM, Wilson CJ (2004) Comparison of IPSCs evoked by spiny and fast-spiking neurons in the neostriatum. J Neurosci 24:7916–7922. CrossRef Medline

Kravitz AV, Kreitzer AC (2012) Striatal mechanisms underlying movement, reinforcement, and punishment. Physiology (Bethesda) 27:167–177. CrossRef Medline

Kyrozis A, Reichling DB (1995) Perforated-patch recording with gramici-din avoids artifactual changes in intracellular chloride concentration. J Neurosci Methods 57:27–35. CrossRef Medline

Lobo MK, Covington HE 3rd, Chaudhury D, Friedman AK, Sun H, Damez-Werno D, Dietz DM, Zaman S, Koo JW, Kennedy PJ, Mouzon E, Mogri M, Neve RL, Deisseroth K, Han MH, Nestler EJ (2010) Cell type-specific loss of BDNF signaling mimics optogenetic control of cocaine reward. Science 330:385–390. CrossRef Medline

Mead AN, Vasilaki A, Spyraki C, Duka T, Stephens DN (1999) AMPA-receptor involvement in c-fos expression in the medial prefrontal cortex and amygdala dissociates neural substrates of conditioned activity and conditioned reward. Eur J Neurosci 11:4089–4098. CrossRef Medline

Mihalek RM, Banerjee PK, Korpi ER, Quinlan JJ, Firestone LL, Mi ZP, Lagenaur C, Tretter V, Sieghart W, Anagnostaras SG, Sage JR, Fanselow MS, Guidotti A, Spigelman I, Li Z, DeLorey TM, Olsen RW, Homanics GE (1999) Attenuated sensitivity to neuroactive steroids in gamma-aminobutyrate type A receptor δ subunit knockout mice. Proc Natl Acad Sci U S A 96:12905–12910. CrossRef Medline

Morris HV, Dawson GR, Reynolds DS, Atack JR, Rosahl TW, Stephens DN (2008) $\alpha2$-containing $GABA_A$ receptors are involved in mediating stimulant effects of cocaine. Pharmacol Biochem Behav 90:9–18. CrossRef Medline

Mortensen M, Ebert B, Wafford K, Smart TG (2010) Distinct activities of GABA agonists at synaptic- and extrasynaptic-type $GABA_A$ receptors. J Physiol 588:1251–1268. CrossRef Medline

Nie H, Rewal M, Gill TM, Ron D, Janak PH (2011) Extrasynaptic δ-containing $GABA_A$ receptors in the nucleus accumbens dorsomedial shell contribute to alcohol intake. Proc Natl Acad Sci U S A 108:4459–4464. CrossRef Medline

Olsen RW, Sieghart W (2008) International Union of Pharmacology. LXX. Subtypes of gamma-aminobutyric acid(A) receptors: classification on the basis of subunit composition, pharmacology, and function. Update. Pharmacol Rev 60:243–260. CrossRef Medline

Paxinos G, Franklin KBJ (2001) The mouse brain in stereotaxic coordinates, Ed 2. San Diego: Academic.

Pirker S, Schwarzer C, Wieselthaler A, Sieghart W, Sperk G (2000) $GABA_A$ receptors: immunocytochemical distribution of 13 subunits in the adult rat brain. Neuroscience 101:815–850. CrossRef Medline

Rewal M, Donahue R, Gill TM, Nie H, Ron D, Janak PH (2012) $\alpha4$ subunit-containing $GABA_A$ receptors in the accumbens shell contribute to the reinforcing effects of alcohol. Addict Biol 17:309–321. CrossRef Medline

Robinson TE, Berridge KC (1993) The neural basis of drug craving: an incentive-sensitization theory of addiction. Brain Res Brain Res Rev 18:247–291. CrossRef Medline

Rudolph U, Knoflach F (2011) Beyond classical benzodiazepines: novel therapeutic potential of $GABA_A$ receptor subtypes. Nat Rev Drug Discov 10:685–697. CrossRef Medline

Santhakumar V, Jones RT, Mody I (2010) Developmental regulation and neuroprotective effects of striatal tonic $GABA_A$ currents. Neuroscience 167:644–655. CrossRef Medline

Sieghart W (2006) Structure, pharmacology, and function of $GABA_A$ receptor subtypes. Adv Pharmacol 54:231–263. Medline

Smith RJ, Lobo MK, Spencer S, Kalivas PW (2013) Cocaine-induced adaptations in D1 and D2 accumbens projection neurons (a dichotomy not necessarily synonymous with direct and indirect pathways). Curr Opin Neurobiol 23:546–552. CrossRef Medline

Taverna S, Ilijic E, Surmeier DJ (2008) Recurrent collateral connections of striatal medium spiny neurons are disrupted in models of Parkinson's disease. J Neurosci 28:5504–5512. CrossRef Medline

van Dongen YC, Deniau JM, Pennartz CM, Galis-de Graaf Y, Voorn P, Thierry AM, Groenewegen HJ (2005) Anatomical evidence for direct connections between the shell and core subregions of the rat nucleus accumbens. Neuroscience 136:1049–1071. CrossRef Medline

Vashchinkina E, Panhelainen A, Vekovischeva OY, Aitta-aho T, Ebert B, Ator NA, Korpi ER (2012) GABA site agonist gaboxadol induces addiction-predicting persistent changes in ventral tegmental area dopamine neurons but is not rewarding in mice or baboons. J Neurosci 32:5310–5320. CrossRef Medline

Wafford KA, van Niel MB, Ma QP, Horridge E, Herd MB, Peden DR, Belelli D, Lambert JJ (2009) Novel compounds selectively enhance δ subunit containing $GABA_A$ receptors and increase tonic currents in thalamus. Neuropharmacology 56:182–189. CrossRef Medline

Walaas SI, Greengard P (1984) DARPP-32, a dopamine- and adenosine 3′: 5′-monophosphate-regulated phosphoprotein enriched in dopamine-innervated brain regions. I. Regional and cellular distribution in the rat brain. J Neurosci 4:84–98. Medline

Watanabe M, Fukaya M, Sakimura K, Manabe T, Mishina M, Inoue Y (1998) Selective scarcity of NMDA receptor channel subunits in the stratum lucidum (mossy fibre-recipient layer) of the mouse hippocampal CA3 subfield. Eur J Neurosci 10:478–487. CrossRef Medline

Wisden W, Laurie DJ, Monyer H, Seeburg PH (1992) The distribution of 13 GABA$_A$ receptor subunit mRNAs in the rat brain. I. Telencephalon, diencephalon, mesencephalon. J Neurosci 12:1040–1062. Medline

Wise RA (2004) Dopamine, learning and motivation. Nat Rev Neurosci 5:483–494. CrossRef Medline

Wlodarczyk AI, Sylantyev S, Herd MB, Kersanté F, Lambert JJ, Rusakov DA, Linthorst AC, Semyanov A, Belelli D, Pavlov I, Walker MC (2013) GABA-independent GABA$_A$ receptor openings maintain tonic currents. J Neurosci 33:3905–3914. CrossRef Medline

Xiao C, Zhou C, Li K, Ye JH (2007) Presynaptic GABA$_A$ receptors facilitate GABAergic transmission to dopaminergic neurons in the ventral tegmental area of young rats. J Physiol 580:731–743. CrossRef Medline

Zimmermann L, Schwaller B (2002) Monoclonal antibodies recognizing epitopes of calretinins: dependence on Ca^{2+}-binding status and differences in antigen accessibility in colon cancer cells. Cell Calcium 31:13–25. CrossRef Medline